UNCLASSIFIED

NRL Report 6333

Radiation Damage in Silicon Solar Cells From 4.6-Mev Proton Bombardment

R. L. STATLER

Electromagnetic Materials Branch
Solid State Division

November 15, 1965

U.S. NAVAL RESEARCH LABORATORY
Washington, D.C.

CONTENTS

Abstract	ii
Problem Status	ii
Authorization	ii
INTRODUCTION	1
EXPERIMENTAL PROCEDURE	2
Solar-Cell Specimens	2
Irradiation and Dosimetry	2
Measurement Techniques	4
RESULTS	7
Current-Voltage Characteristics	7
Diffusion Length	8
Photovoltaic Spectral Response	9
CONCLUSIONS	10
ACKNOWLEDGMENTS	11
REFERENCES	11

Copies available from Clearinghouse for Federal Scientific
and Technical Information (CFSTI) Sills Building,
5285 Port Royal Road, Springfield, Virginia 22151
$2.00

ABSTRACT

A study has been made of the radiation damage in ten types of silicon solar cells as a result of 4.6-Mev proton bombardment. The cells comprised such types as p/n cells, n/p cells with different bulk-resistivities, planar cells, and drift-field cells. A comparative analysis was made of the radiation-induced degradation in these cells as a function of short-circuit current, maximum power output, minority-carrier diffusion length, and photovoltaic spectral response. The p/n cells were found to be more sensitive to radiation damage than any type of n/p cell in this study. In the n/p cells, there is a definite trend toward increasing radiation resistance accompanying increasing values of bulk resistivity, up to 10 ohm-cm. The drift-field solar cells exhibit a further improvement in radiation resistance beyond that of the other types of n/p cells.

PROBLEM STATUS

This is a final report on one phase of the problem; work is continuing on other phases of the problem.

AUTHORIZATION

NRL Problem E02-04
BuShips Projects SF-013-12-04-4533
and SR-007-11-01-0549
NASA Projects S-13991-G and S-4757-G

Manuscript submitted July 28, 1965.

RADIATION DAMAGE IN SILICON SOLAR CELLS FROM 4.6-MEV PROTON BOMBARDMENT

INTRODUCTION

Silicon photovoltaic cells have been used as the sole source of electrical energy for all space vehicles whose active lifetimes were longer than that which could be provided by batteries. The discovery in 1958 of the presence of large fluxes of charged-particle radiation within the earth's geomagnetic field stimulated much interest in the effects of radiation on solar cells. The cells as used on satellites are shielded only from lower energy particles by transparent materials whose thickness must be limited by weight restrictions. As a result, the higher energy electrons and protons penetrate the shielding and bombard the solar cells. The general consequence of this radiation exposure is manifested as a gradual decrease in output power until satellite data acquisition and transmission are stopped.

This situation has established the need for determining with greater precision and detail the radiation damage to types of solar cells in current use or development for operation in radiation environments. Furthermore, there is a great need to discover which parameters of solar-cell design or materials are critically related to radiation resistance.

A previous study (1) of 1-Mev electron bombardment damage in silicon solar cells demonstrated that n/p cells are more resistant to damage than p/n cells. At the same time, p-type silicon of higher resistivity was observed to be less damaged than low-resistivity silicon (about 1 ohm-cm) for the same exposure dose. In keeping with these results, and mindful of the different damage mechanisms produced by proton bombardment, a research program was undertaken with the following objectives:

1. To study comparative radiation damage from protons on n/p solar cells commercially available from sources capable of supplying quantity lots from regular production runs.

2. To include in the comparative investigation a representative type of commercial p/n cell.

3. To examine the relationship between solar-cell base resistivity and radiation damage rate in a quantitative manner.

4. To employ a sufficient number of each type of cell so as to ensure statistically meaningful data.

5. To include several experimental types of solar cells which have a theoretical basis for exhibiting improved radiation resistance characteristics; e.g., solar cells of the drift-field and planar type.

6. To minimize the number of experimental variables in the radiation exposure by making exposure doses as uniform and equal as possible and by keeping all cells in a similar nonradiative environment.

7. To ensure accuracy and reproducibility in all measurements through the frequent use of calibrating standards.

EXPERIMENTAL PROCEDURE

Solar-Cell Specimens

The solar cells used in this study were procured by the Spacecraft Technology Branch of the Goddard Space Flight Center, National Aeronautics and Space Administration. In October 1962, all known solar-cell manufacturers were requested to supply lots of 100 n/p silicon cells from their regular production. Each cell was required to have an efficiency of at least 10 percent as measured under a water-filtered 2800°K tungsten light source. Six companies fulfilled the request and furnished cells made from p-type silicon having a nominal resistivity of either 1 or 10 ohm-cm. Furthermore, one lot of 100 p/n solar cells with a nominal base resistivity of 1 ohm-cm was obtained from a major supplier. These cells were chosen for the large amount of existing data on an established type which was representative of the current state of development in this field. Each of the cells was examined with regard to its current-voltage (I-V) characteristics. The 15 cells in each group of 100 which had I-V values closest to the median of each respective lot were chosen for an electron-bombardment experiment (1). The next lot of 15 cells in each group which had I-V values closest to the median was chosen for the present investigation. However, only six samples selected at random from each group were proton-irradiated.

In addition to these commercial cells, three groups of experimental solar cells were included in the study. The first group comprised six n/p planar solar cells, so designated because the techniques conventionally employed in the manufacture of planar semiconductor devices were adapted to their fabrication. Accordingly, the p-n junction is diffused into the surface through a silicon oxide layer which serves a dual purpose. It prevents the edge of the p-n junction from being a region of high dislocation density, and it forestalls the possibility of surface contamination. Both conditions are possible in the conventional manufacture of solar cells, when the exposed junction edges are lapped or etched after the diffusion process is completed.

Next, there were two groups of cells furnished by another supplier, both of which were made from p-type silicon having a resistivity of 25 ohm-cm, and were prepared by conventional techniques, with the following exception: one of these groups of cells comprised the so-called "drift-field" cells. These cells are made by first diffusing a donor-type impurity from the rear surface such that a variation of impurity concentration is achieved along the direction normal to the face. The p-n junction is then diffused in the normal manner from the front surface. The first diffusion process creates an internal electric field which is proportional to the gradient of the impurity concentration. The net effect of the drift-field process is to accelerate minority carriers toward the junction and thus to increase the probability for carriers to be collected at the junction before recombination capture can occur.

A detailed list of the specimen cells grouped according to type is presented in Table 1. A photograph of the cells is shown in Figure 1.

Irradiation and Dosimetry

The bombardment of the cells was performed in the NRL 5-Mev Van de Graaff accelerator. The horizontal beam from this machine was scattered by a 0.0004-in.-thick gold foil placed in the drift tube about 18 ft from the solar-cell mounting block. This foil served the dual purpose of reducing the beam intensity and of providing a more uniform flux distribution over the target area. The energy of the incident protons on the foil was measured as 5.127 Mev. The calculated energy of the beam after scattering through the foil was 4.6 Mev. At this energy the range of protons in silicon is about 150 microns, which is close to the value of the minority-carrier diffusion length in most of the solar cells before irradiation.

Table 1
Solar-Cell Specimens Used in the Experiment

Group*	Resistivity (ohm-cm)	Type †	Active Area‡ (cm^2)
A	1	p/n, com.	1.78
B	1	n/p, planar, exp.	3.60
C	1	n/p, com.	1.80
D	1	n/p, com.	1.70
E	25	n/p, exp.	0.85
E_{DF}		n/p, drift field, exp.	0.85
F	10	n/p, com.	1.78
G	10	n/p, com.	1.79
H	1	n/p, com.	1.80
K	1	n/p, com.	1.69

*All groups were composed of six cells each
†com. = commercial; exp. = experimental
‡The active area includes the surface covered by the fine grid lines of the cell but excludes the surface covered by the main grid strip.

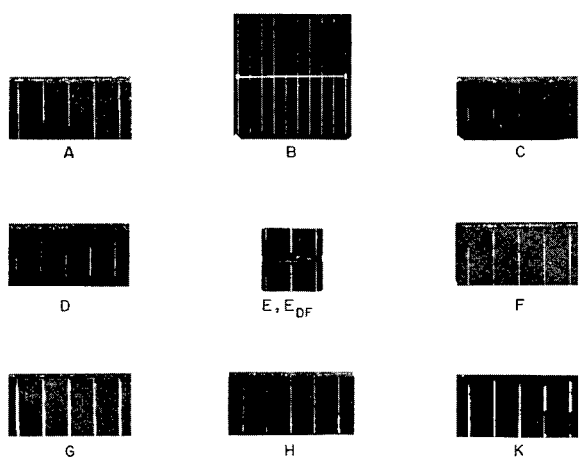

Fig. 1 - The nine configurations of solar cells used in this experiment

The flux was measured by a Faraday cup technique, as illustrated by the diagram in Fig. 2. A beam-defining aperture was placed in the drift tube just prior to the final tube section, which was electrically insulated from the rest of the assembly. The proton beam passing through the aperture was measured and recorded by an integrating electrometer circuit.

The uniformity of flux distribution over the specimen area was determined by using a specially designed target block on which four copper rectangles, measuring 1×2 cm, were

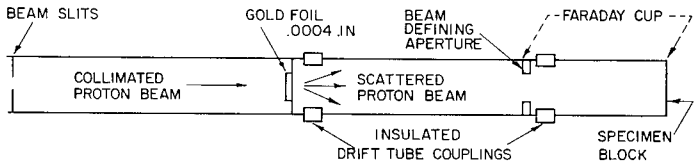

Fig. 2 - Schematic representation of the Van de Graaff drift-tube assembly

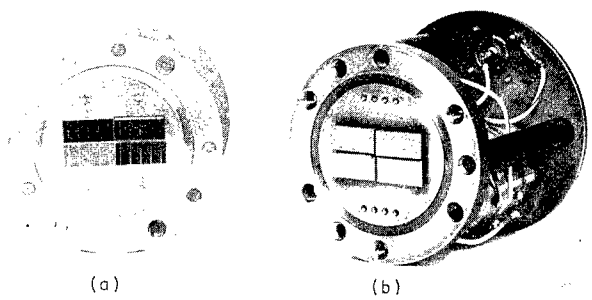

Fig. 3 - The solar-cell mounting block (a) and the flux-distribution monitoring block (b)

soldered to Stupakoff feed-throughs. The proton beam collected by each copper plate was measured, and the resultant values indicated a flux deviation of ±1 percent from the average. The solar cells, irradiated four at a time, were held against the specimen block by spring-wire fingers against the grid strips. Figure 3 shows the mounting of the solar cells and the flux-measuring target block. The flux integration was carried out prior to the bombardments in order to establish the time for the desired exposure doses, and also during each cell-group bombardment. The variation in the integrated flux values from one group of cells to another was within ±1.3 percent.

Measurement Techniques

Current-Voltage Characteristics – The cells were bombarded in accordance with the irradiation schedule presented in Table 2. Prior to the bombardment and following each incremental dose, the I-V characteristic was obtained for each cell under illumination by a tungsten light source. This light source, the same type as used to select the specimen cells for the experiment, consisted of a 300-watt reflector flood bulb carefully calibrated to a color temperature of 2800°K. Thereafter the lamp voltage was controlled by means of an electric voltage regulator to within 0.2 volt, with a corresponding variation in color temperature of only ±2°K. A heat-absorbing filter comprising a 3-cm thickness of deionized water contained in a methyl methacrylate holder with 0.25-in. walls was interposed in the light path. The light intensity incident on the cell holder was measured by observing the short-circuit current output of a reference solar cell placed in the holder. In order to achieve this purpose, ten n/p solar cells (supplied by Western Electric) were measured in succession prior to recording the I-V curves of the bombarded cells. The light intensity at the test plane was adjusted as required by simply locating the cell holder at a distance from the lamp such that the short-circuit current of the reference solar cells was equivalent to that produced by a sunlight intensity of 100 milliwatts/cm^2.

Table 2
Exposure Dose for Solar-Cell Specimens

Exposure Dose (protons/cm^2)	Number of Cells Exposed in Each Group*		
	E	E_{DF}	All Others
10^{10}	6		6
2.2×10^{10}	6	6	
3×10^{10}	6		6
6.5×10^{10}	6	6	
10^{11}	6		6
2.1×10^{11}	6	6	
3×10^{11}	6		6
8×10^{11}	6	6	

*Following each increment of bombardment, measurements were performed on each group of cells as explained in the text.

The I-V characteristics of the irradiated cells were then plotted automatically, on an X-Y recorder, while a continuously variable resistive load was inserted across the solar-cell terminals. The short-circuit current and the open-circuit voltage were measured independently by voltage-to-frequency conversion techniques. The limit of accuracy of the short-circuit current (I_{sc}) data was ±0.1 ma for all cells in the study. The above data served as the basis for the calculation of the short-circuit current density and the maximum power output.

Diffusion Length – The effect of proton bombardment on the minority-carrier diffusion length of the solar cells is a problem of particular interest and importance. It is known (2) that the diffusion length is especially sensitive to radiation damage, even more so than are the I-V characteristics. Another advantage inherent in the diffusion-length measurement is its essential independence of the surface condition of the cell as well as the p-n junction depth, both of which influence the photovoltaic properties of the cell. From among the wide variety of methods for the measurement of diffusion length in semiconductor devices (3), a particular technique referred to as "the electron-injection technique," reported by Rosenzweig (4), was used for the present investigation. This method is based on the fact that ionizing radiation may be used to generate excess carriers at a known rate in a semiconductor. The radiation-generated short-circuit current may then be used to calculate diffusion lengths when the device geometry is known.

In the present application, the electron injection is accomplished by measuring the short-circuit current generated in the cell by a low-intensity 1-Mev electron beam. The details of this measurement have been described elsewhere (1,4). The diffusion length is found to be

$$L = J_{sc} / J_e S_o \tag{1}$$

where

L = diffusion length

J_{sc} = short-circuit current density

J_e = beam current density

S_o = carrier generation rate (numerically equal to 225 pairs per micron for each incident 1-Mev electron)

The diffusion length was measured at the beginning of the experiment and following each bombardment of three cells selected randomly from each of the seven commercial types. The unusual dimensions and grid patterns of the experimental cells precluded their accommodation in the special Faraday cup.

Photovoltaic Spectral Response – A third perspective of radiation damage in solar cells is afforded by an examination of the change in photovoltaic spectral response. This parameter may generally be described as the functional dependence of the solar-cell short-circuit current response on the wavelength of incident light. More specifically, the quantum efficiency, which is closely related, is defined as the fractional number of liberated minority carriers which diffuse to the junction per incident photon. This fraction is, of course, dependent on the photon energy or wavelength. The general characteristics of the wavelength dependence in a solar cell are well known, exhibiting a falling off of the response at both short and long wavelengths. At short wavelengths, the carrier generation is predominantly localized in the region close to the cell surface, where the minority-carrier lifetime is extremely short. Hence, the collection efficiency for carriers from this region is small. On the other hand, light of longer wavelength generates a substantial number of carriers within the bulk of the cell at a distance exceeding the bulk minority-carrier diffusion length. Again, the result is a reduction in collection efficiency for these carriers.

In this present experiment, the spectral response of all of the cells for which diffusion-length measurements were made was observed. A modification of the spectral-response apparatus developed at NRL (5) was utilized (Fig. 4).

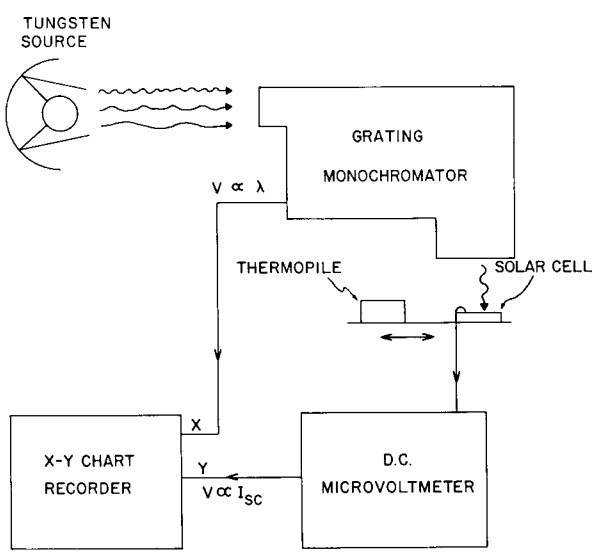

Fig. 4 - Block diagram of the photovoltaic spectral response apparatus

RESULTS

Most of the results will be presented in detail sufficient to reveal many of the small but significant differences in radiation damage in different types of cells. Since much of the data are self-explanatory, some aspects of the work will not require detailed discussion. Instead, important and meaningful conclusions applicable to a type of solar cell will be emphasized.

Current-Voltage Characteristics

The I-V characteristics are presented in Figs. 5 through 14.* The extreme values of this parameter are exhibited for the cell specimens in each group, with the exception of group B. Since this is an experimental cell requiring more complex fabrication and utilizing smaller lots, it was expected to show less uniformity. Thus only the data for a single cell of this type are presented (Fig. 6).

It is recalled that the specimen cells were selected from a larger group of cells on the basis of having short-circuit currents close to the median value of each respective group. Nevertheless, it is seen that uniformity in the value of I_{sc} does not guarantee that the cells will degrade uniformly under proton bombardment (Figs. 5, 8, 10, 14). Four groups of solar cells show an increasing spread in I_{sc} with increasing exposure doses.

An examination of the I-V characteristics reveals the degree of nonuniformity existing among solar cells within the same group. The observed inhomogeneity emphasizes the difficulties inherent in a complex fabrication process for semiconductor devices. It is probable that variations in impurity concentration and dislocation density in the parent crystal may give rise to erratic behavior of p-n junction devices.

The short-circuit current densities J_{sc} were obtained from the foregoing data (Figs. 15 through 24). Extreme values for each group are shown at each bombardment level. The values of J_{sc} were computed by dividing the observed values of I_{sc} by the active cells areas as given in Table 1.

The initial current densities of the commercial solar cells fall in the range of 26.8 to 29.3 ma/cm^2. The narrowness of these limits implies that the junction diffusion and surface-coating technologies throughout the solar cell industry have attained the same level of achievement. The current densities of the experimental cells are somewhat lower, falling into a range of 22.3 to 25.8 ma/cm^2.

The rates of short-circuit current degradation may be more easily compared by calculating the percentage of initial current remaining at the end of each bombardment (Figs. 25 through 34). These graphs show that the damage rate for I_{sc} is approximately 20 percent per decade of dose for 1-ohm-cm cells, 16 percent per decade for the 10-ohm-cm, and 20 percent per decade for the 25-ohm-cm specimen. The drift-field cell (Fig. 30) showed a marked difference from other types in damage-rate behavior. The damage rate does not appear to approach a constant value, as is the usual case, but becomes increasingly larger with bombardment dose.

A summary of the I_{sc} results is shown in Fig. 35, wherein is presented the relative order of damage rates for each type of cell. These data facilitate the determination of the integrated flux required to produce a 25-percent decrease in the unirradiated I_{sc} value for each type. The appropriate flux values as well as the flux ratios are listed in Table 3. The flux ratio is obtained by dividing the integrated flux, Φ_c, of 4.6-Mev protons

*Figures 5 through 61 are bound consecutively at the end of the text.

Table 3
The Integrated Flux, Φ_c, of 4.6-Mev Protons Required to Degrade the Short-Circuit Current of Various Types of Solar Cells to 75 Percent of the Original Value

Cell Type*	Φ_c (p/cm^2)	Flux Ratio
p/n, 1 ohm-cm, com.	1.06×10^{10}	1
n/p, 1 ohm-cm, com.	7.5×10^{10}	7
n/p, 10 ohm-cm, com.	1.37×10^{11}	13
n/p, 25 ohm-cm, exp.	1.63×10^{11}	15
n/p, drift field, exp.	5.7×10^{11}	54

*Com. = commercial; exp. = experimental.

Note: The solar-cell current is generated by water-filtered tungsten light with a color temperature of 2800°K. The Φ_c for each type of n/p cell is divided by the Φ_c for the p/n cell and expressed as a flux ratio.

required to degrade the short-circuit current of a solar cell to 75 percent of the preirradiation value by the corresponding Φ_c value for the p/n 1-ohm-cm commercial type of cell. Thus the flux ratios for the various kinds of cells are a measure of the relative radiation resistance. It is evident that the cells may be grouped according to resistivity. From the point of view of flux ratios, the superiority of all of the n/p cells over the commercial p/n type is clearly established. It is also noted that an increase in resistivity of the bulk material accompanies an increasing resistance to radiation damage in the range of resistivities considered.

A factor of greater importance than short-circuit current attainable in a solar-cell power system is the residual power-producing capability following radiation bombardment. The dependence of the maximum power density on the integrated flux is shown in Figs. 36 through 45. The power-damage rate for 1-ohm-cm cells is 23 percent per decade of integrated flux and approximately 20 percent per decade for the 10-ohm-cm cells. Both 25-ohm-cm cells and the drift-field cells reveal an increased falling off of power-production capability at the high-exposure doses. The above results emphasize the need to examine the power degradation as well as the change in short-circuit current output when assessing radiation damage in solar cells. The results for radiation damage are summarized in Table 4, which shows the relative doses required to degrade specific types of solar cells to arbitrarily assigned values of J_{sc} and P_{max}.

Diffusion Length

Minority-carrier diffusion-length measurements for three randomly chosen cells of each commercial type were carried out at the outset of the experiment and following each incremental bombardment. The observed average values are plotted as a function of the integrated flux, as shown in Figs. 46 through 52. The theoretical treatment of diffusion-length degradation predicts a straight-line relationship on a log-log plot, where the slope of the line is -1/2. This predicted behavior is verified by the data from all of the 1-ohm-cm specimens, whether they are p/n or n/p type. Some divergence from the above value of slope is noted for the F group of 10-ohm-cm cells. The inference from these data is that the radiation behavior of this group of cells cannot be completely described by the theoretical relationship stated above.

Table 4
The Relative Exposure Dose of 4.6-Mev Protons Required to Degrade Certain Types of Solar Cells to Specified Values of J_{sc} and P_{max}

Cell Type	Relative Exposure Dose for the Specified Values of J_{sc} and P_{max}		
	J_{sc} = 19ma/cm^2	P_{max} (1) = 7mw/cm^2	P_{max} (2) = 6mw/cm^2
1 ohm-cm, n/p	6 to 12	2 to 15	2 to 5
10 ohm-cm, n/p	13 and 30	10 and 15	13 and 18
25 ohm-cm, n/p	10	3	4
Drift field, n/p	11	14	14

NOTE: Relative dose is expressed as a multiple of the dose required to degrade the p/n cells to the respective values.

A summary of the foregoing data is presented in Fig. 53. Reference to the curves supports the conclusions derived from the I-V characteristics with regard to the order of radiation resistance of the cells. Thus all of the n/p cells in this study are superior to the p/n cells, from the point of view of retaining long diffusion lengths, and also the 10-ohm-cm cells show less damage than the 1-ohm-cm specimens on the same basis.

Figure 54 is a graphical representation of the damage constant K, defined by

$$K = d(1/L^2)\,d\Phi \tag{2}$$

where

K = damage constant (a function of the material, the resistivity, the temperature, and the type and energy of the bombarding particle)

L = minority-carrier diffusion length

Φ = integrated radiation flux

The K value provides a convenient measure for gaging relative radiation damage among various types of solar cells. Furthermore, it affords a useful index for assessing the wide range of damage rates produced in a given type of cell by diverse radiation fields.

The value of the damage constant for the group D solar cells reported here agrees closely with that reported by Rosenzweig (6). This constitutes a measure of the accuracy of the present flux determinations and of the diffusion-length measurements.

Photovoltaic Spectral Response

The relative photovoltaic spectral response was obtained for the same cells which were included in the diffusion-length measurements. The measured values of spectral response are used in the calculation of quantum efficiency in the following manner. First, the relative response is normalized on the basis of constant illumination intensity; next, the normalized response is divided by the number of photons represented by the light energy at each wavelength.

The above results are reported in Figs. 55 through 61. Data from only one cell are reported for each group; the cell whose response is closest to the average of the group was selected for illustration.

A study of the curves shows the well-known decrease in the long-wavelength response which is characteristic of bulk-radiation damage and its effect on minority-carrier diffusion length. In general, the spectral-response data do appear to confirm the results obtained on silicon solar cells in the other types of measurements reported above.

CONCLUSIONS

This quantitative study of radiation damage in silicon solar cells from 4.6-Mev proton bombardment has been giving greater perspective by utilizing three avenues of approach, namely, study of I-V characteristics, diffusion-length measurements, and photovoltaic spectral responses. The results confirm that each method is in itself sufficiently sensitive and reliable to provide a basis whereby the radiation resistance of various cell types can be compared. However, the three aspects of radiation damage when viewed collectively provide a more complete understanding of the effects of proton bombardment. A close examination of the results derived from each of the methods discloses a high degree of correlation and thus confirms the accuracy of the conclusions and the confidence to be placed in each technique. An example is the close agreement between the values of diffusion length and short-circuit current density in the 1-ohm-cm n/p cells.

A definition of radiation resistance for solar cells which receives universal acceptance as a suitable criterion under all environmental and engineering conditions is not simple to formulate. Each solar-cell user has a specific requirement in his system which will be a critical operational parameter. For example, the percentage change in short-circuit current may in one case be more important than the change in maximum power, or a limit may be fixed on the amount of permissible variation in one of these parameters. Again, the individual user may be primarily interested in retaining a certain minimum level of spectral response at particular wavelengths. Since it is not possible to combine all these factors into a single standard, it is considered advisable to present all results in sufficient detail so that further analysis of the data can be performed if required.

From the practical standpoint, that a satellite must be supplied with a minimum level of power to maintain continuous operation, it would appear that an arbitrary value of power-output density should be proposed as an index of radiation damage. Even so, the relative radiation resistance of the cells remains a function of the particular power level which is chosen.

With such a criterion, the following specific conclusions are stated:

1. The 1-ohm-cm p/n cell is definitely less radiation resistant to 4.6-Mev proton bombardment than any of the n/p types. This is evident in all the measured parameters.

2. The 1-ohm-cm n/p groups from different manufacturers are quite uniform with respect to damage rates, and can be classed as a single type. Small deviations which appear can be attributed to variations in the bulk resistivity of the cell, where higher resistivity is indicative of greater radiation resistance.

3. The 10-ohm-cm n/p cells display a greater resistance to radiation damage than the 1-ohm-cm cells. The reason for the difference in the slope of the diffusion-length-degradation curves of the two groups of 10-ohm-cm cells is not understood.

UNCLASSIFIED

4. The radiation resistance of the experimental 25-ohm-cm cell cannot be validly compared with the commercial n/p cells on the basis of arbitrary power output, because the group E cells are initially much less efficient than the commercial cells. While the E group cells have a lower power output following the final bombardment than do the commercial cells, they have a smaller percentage change in power from the initial to the final stages.

5. A comparison of the 25-ohm-cm and drift-field cells, of almost equal initial efficiencies, shows a decided improvement for the drift-field cell. Additional study of the drift-field effect as applied to solar cells appears to be well warranted.

ACKNOWLEDGMENTS

The author wishes to thank Messrs. W. Cherry and M. Schach of Goddard Space Flight Center, NASA, for their continual interest and support of this experiment. Thanks are due Mr. K. Dunning and his staff of the Van de Graaff Branch, Nucleonics Division, for providing the use of the 5-Mev accelerator and facilities. The author is grateful to his many colleagues who so ably assisted in this study.

REFERENCES

1. Statler, R.L., "Electron-Bombardment Damage in Silicon Solar Cells," NRL Report 6091, Oct. 7, 1964

2. Rosenzweig, W., Gummel, H.K., and Smits, F.M., Bell System Tech. J. 42:399 (1963)

3. Bemski, G., Proc. IRE 46:990 (1958)

4. Rosenzweig, W., Bell System Tech. J. 41:1573 (1962)

5. Flesch, J.P., and Statler, R.L., "Thermal, Mechanical, and Environmental Characteristics," Report of NRL Progress, p. 31, June 1962

6. Rosenzweig, W., Smits, F.M., and Brown, W.L., J. Appl. Phys. 35:2707 (1964)

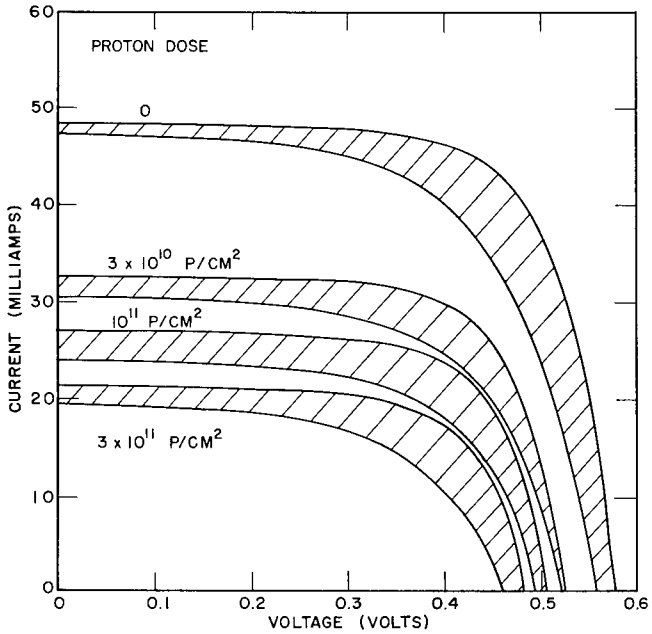

Fig. 5 - I-V characteristic of group A solar cells as a function of proton dose. The widths of the bands illustrate the limits of variation observed in individual cells

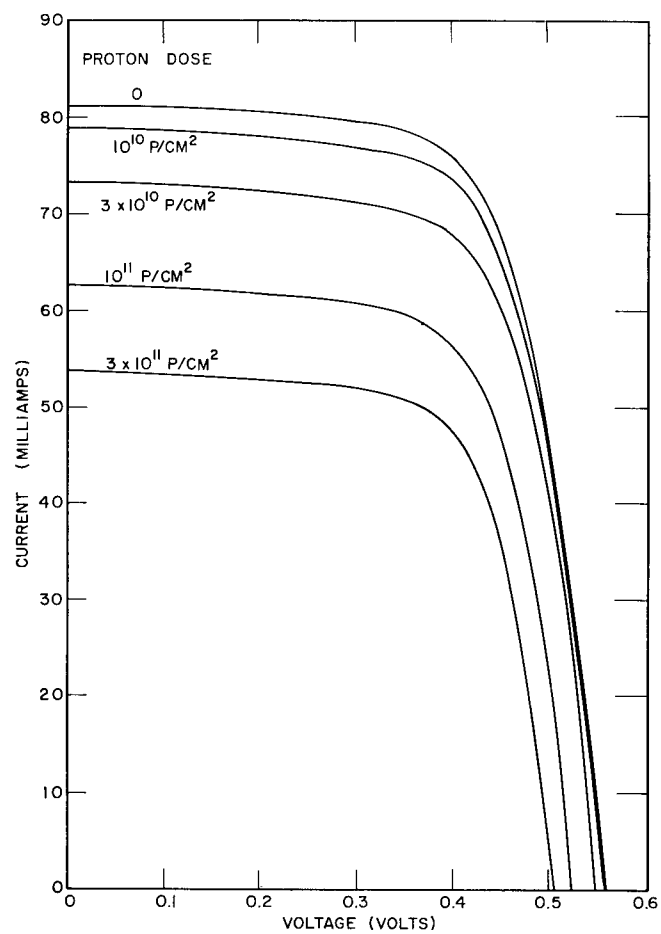

Fig. 6 - I-V characteristic of a representative group B solar cell

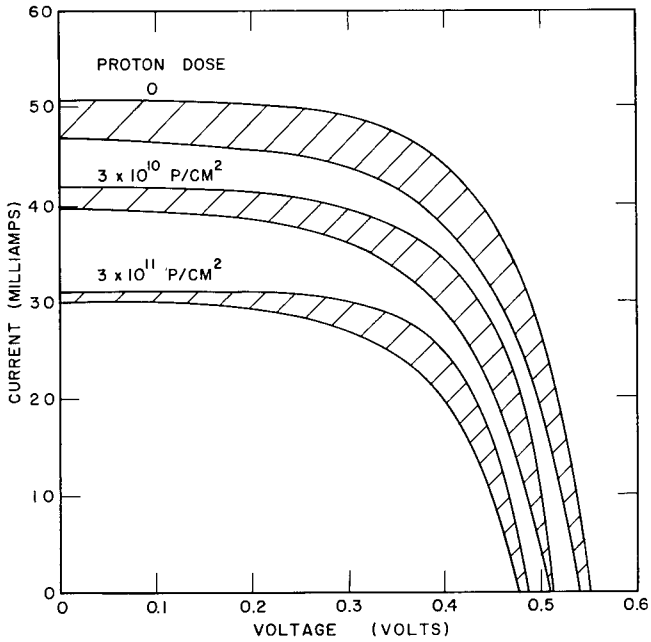

Fig. 7 - I-V characteristic of group C solar cells

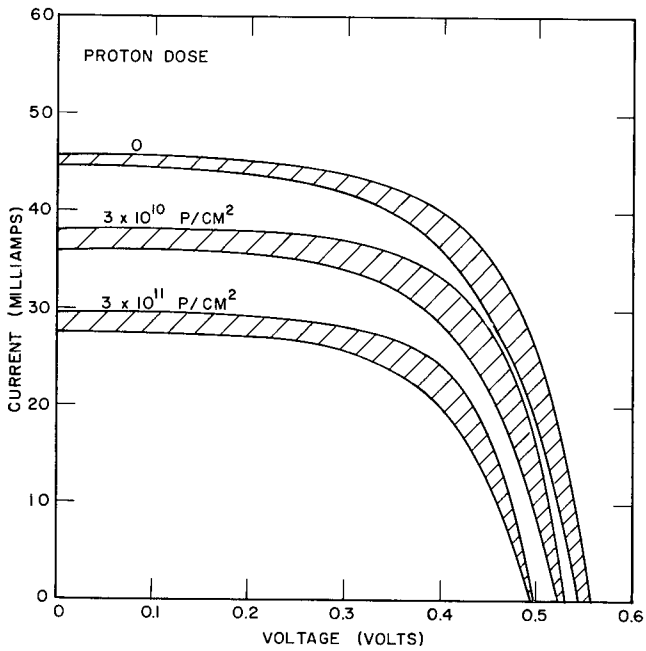

Fig. 8 - I-V characteristic of group D solar cells

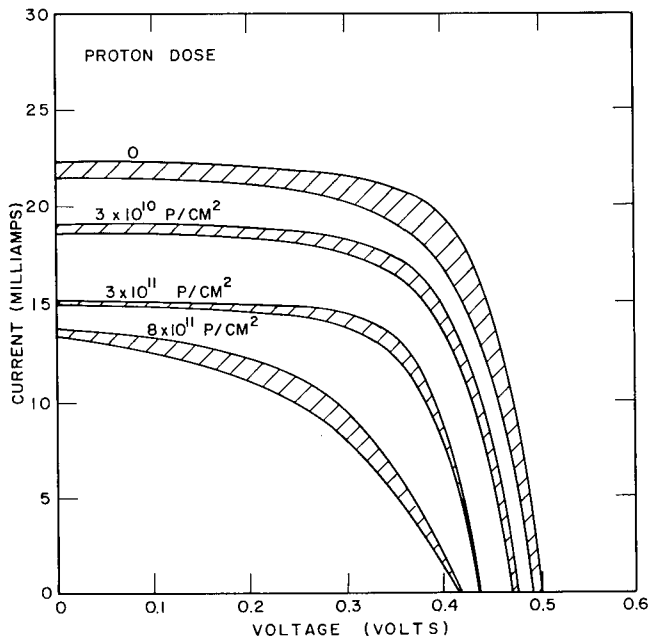

Fig. 9 - I-V characteristic of group E solar cells

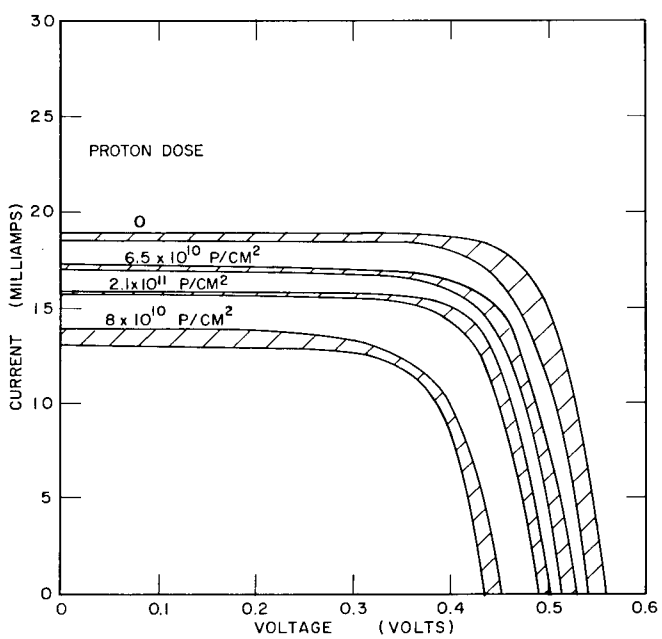

Fig. 10 - I-V characteristic of group E_{DF} solar cells

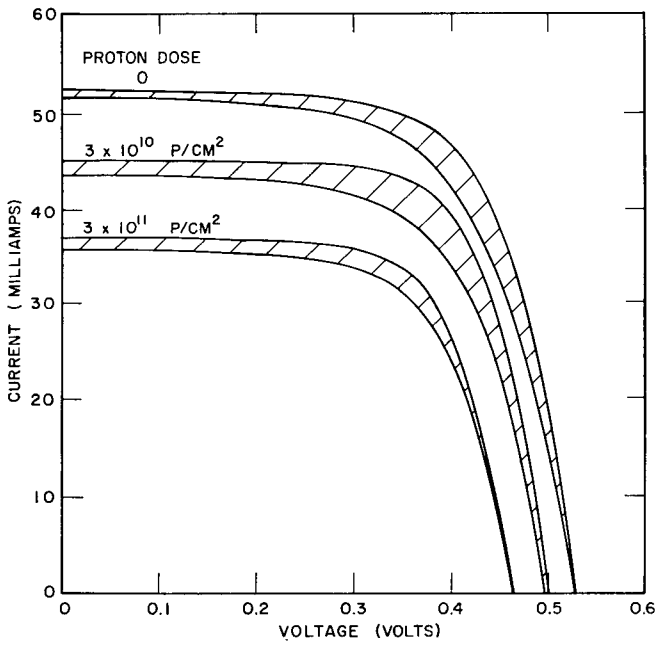

Fig. 11 - I-V characteristic of group F solar cells

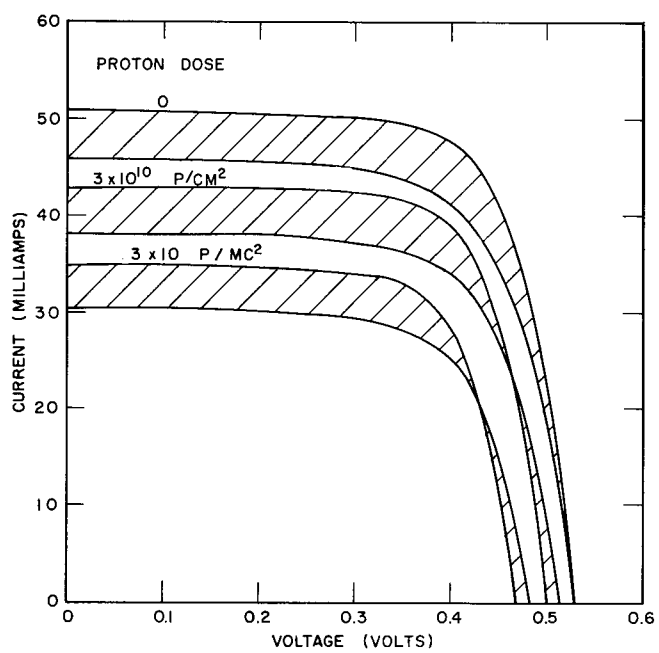

Fig. 12 - I-V characteristic of group G solar cells

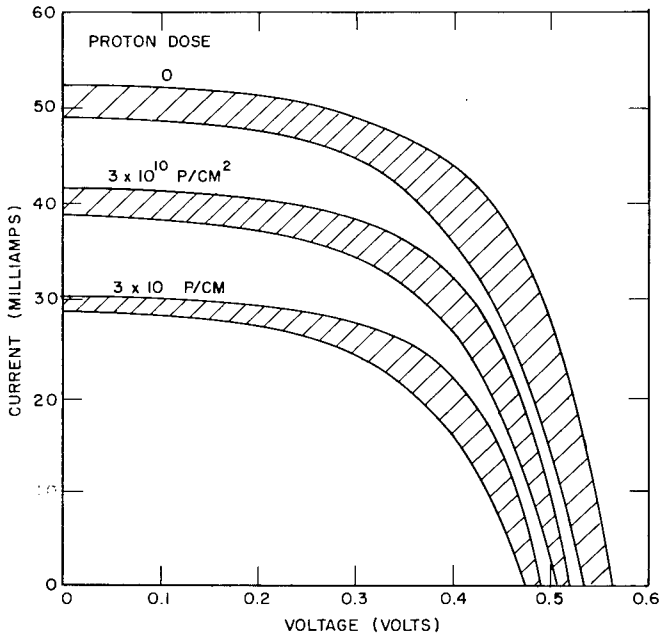

Fig. 13 - I-V characteristic of group H solar cells

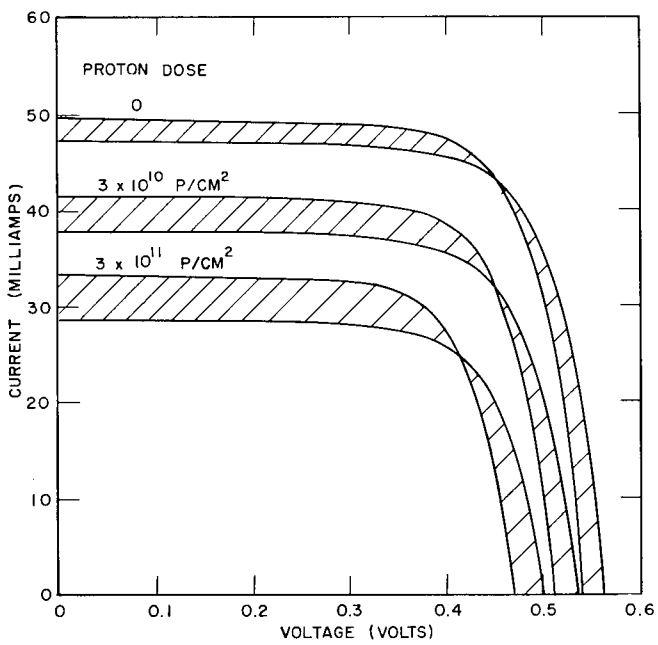

Fig. 14 - I-V characteristic of group K solar cells

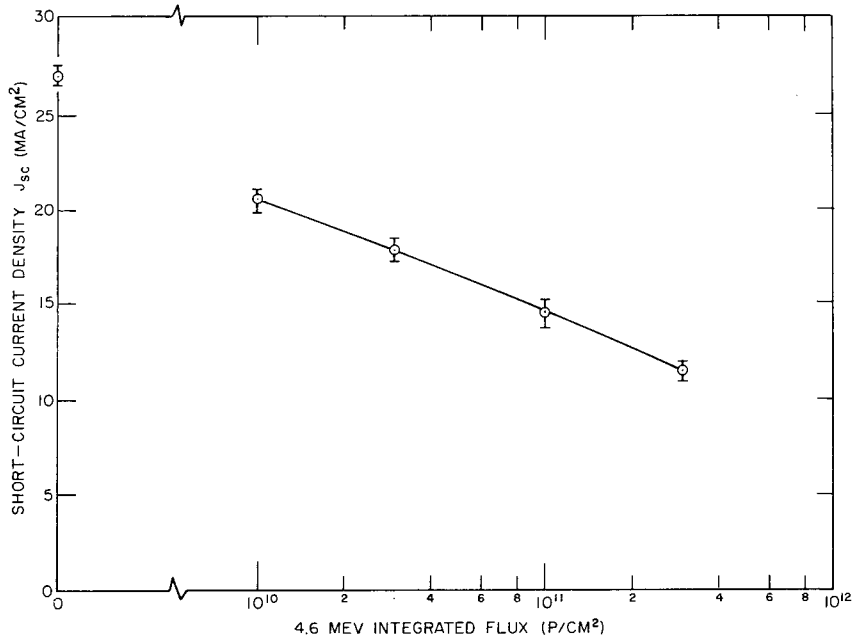

Fig. 15 - Short-circuit current density J_{sc} of group A solar cells after proton bombardment. The median and extreme values are shown.

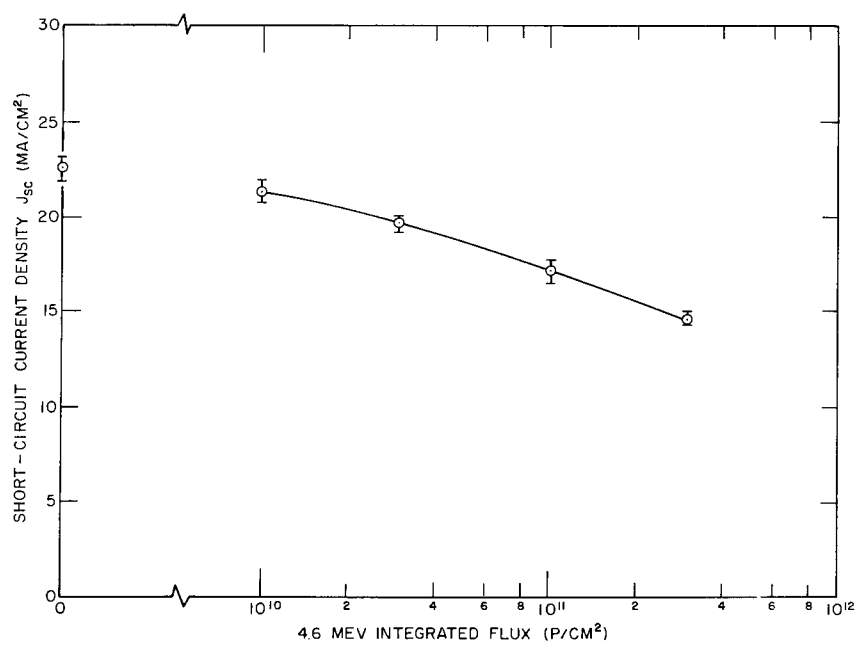

Fig. 16 - Short-circuit current density J_{sc} of group B solar cells

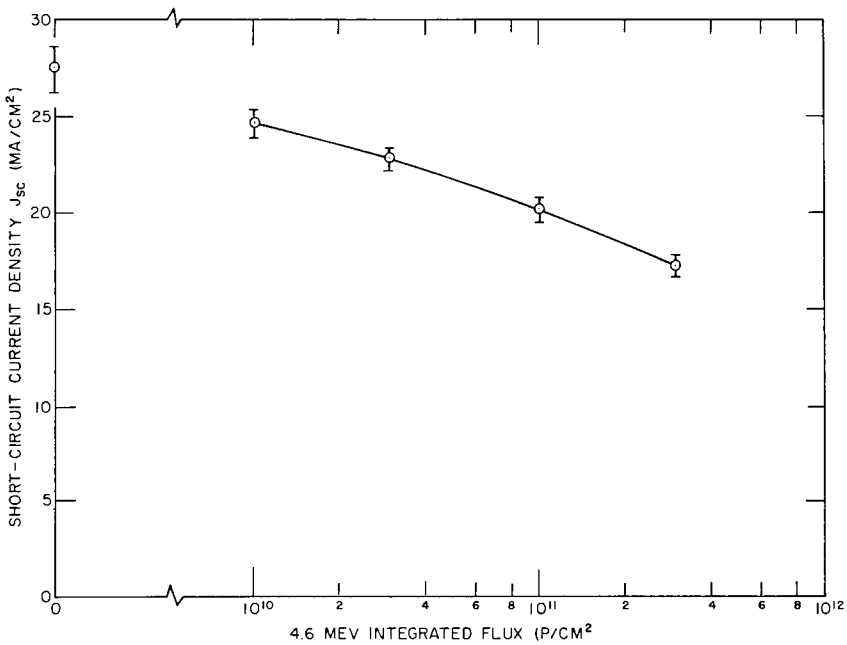

Fig. 17 - Short-circuit current density J_{sc} of group C solar cells

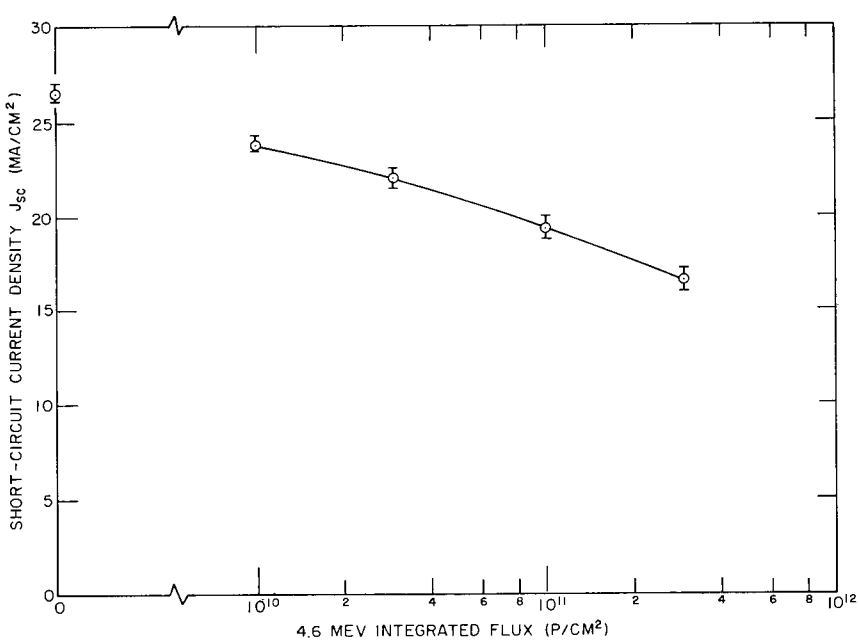

Fig. 18 - Short-circuit current density J_{sc} of group D solar cells

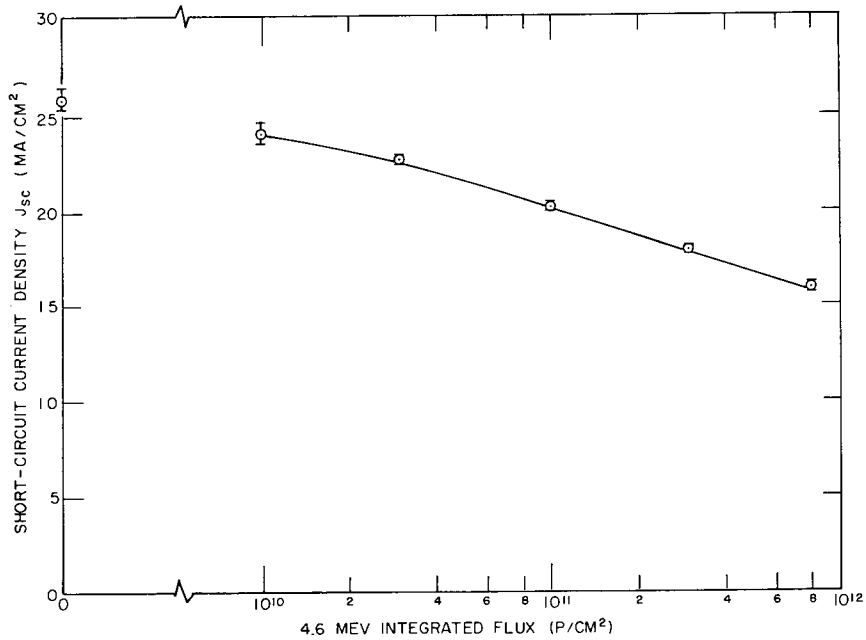

Fig. 19 - Short-circuit current density J_{sc} of group E solar cells

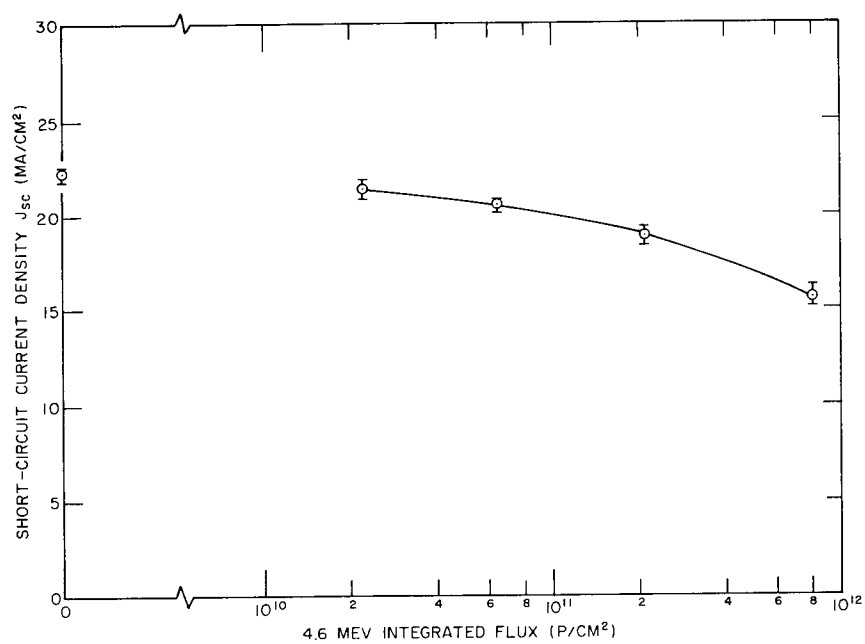

Fig. 20 - Short-circuit current density J_{sc} of group E_{DF} solar cells

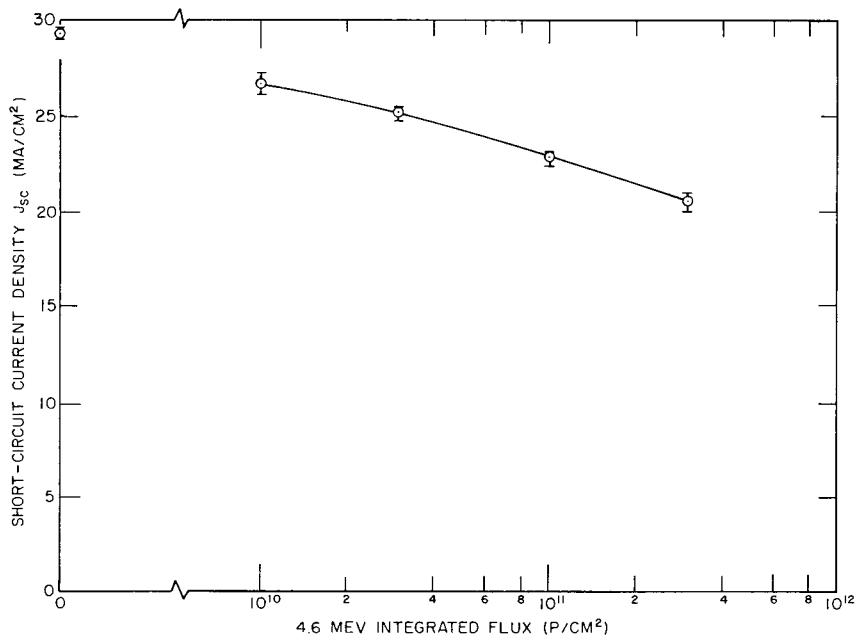

Fig. 21 - Short-circuit current density J_{sc} of group F solar cells

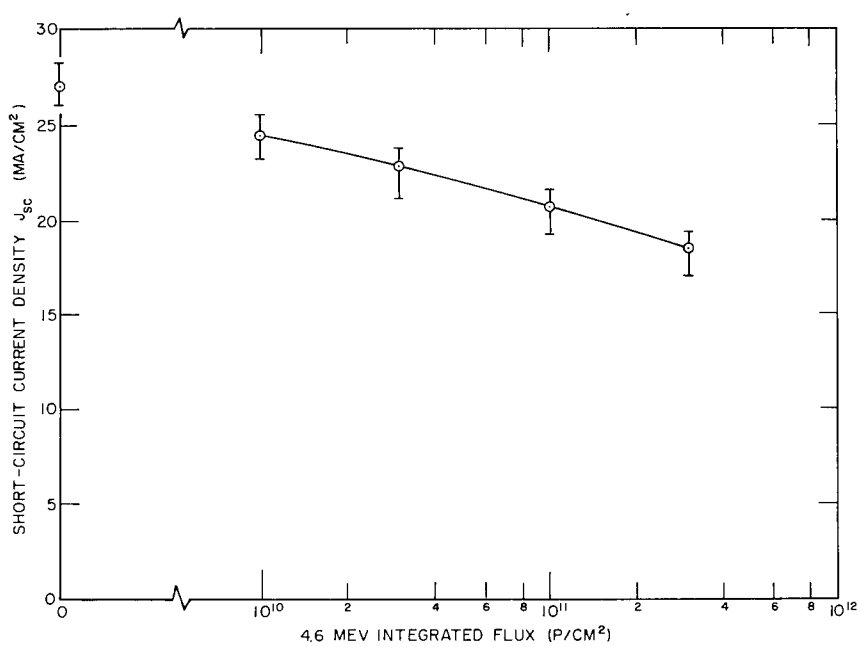

Fig. 22 - Short-circuit current density J_{sc} of group G solar cells

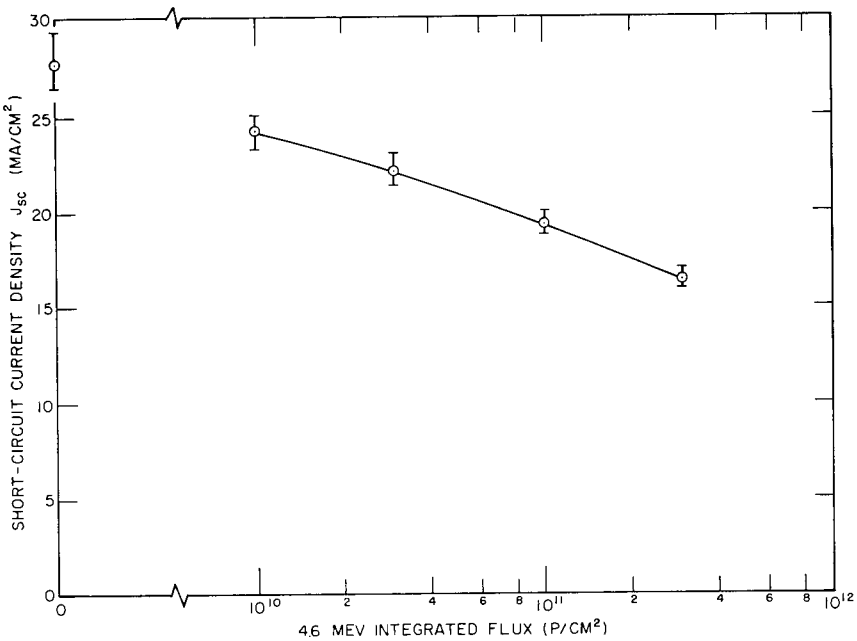

Fig. 23 - Short-circuit current density J_{sc} of group H solar cells

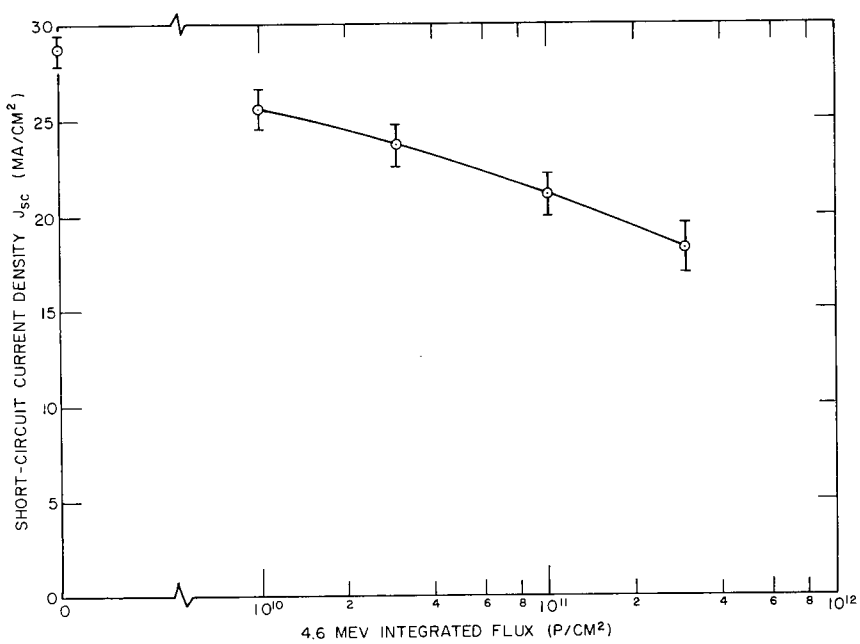

Fig. 24 - Short-circuit current density J_{sc} of group K solar cells

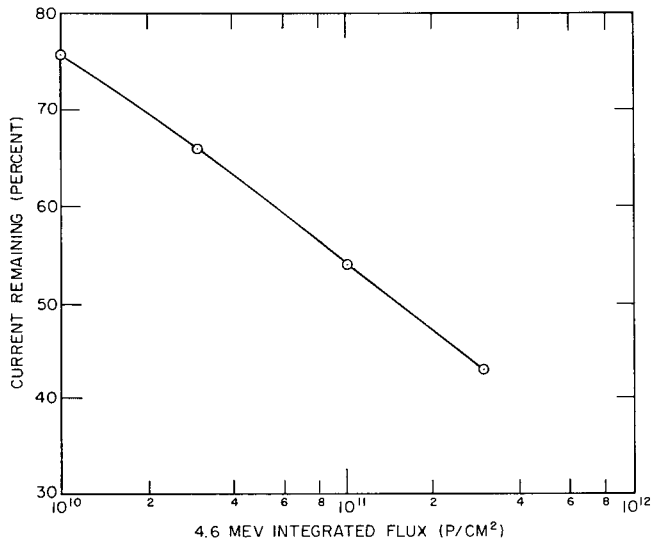

Fig. 25 - Percentage change in short-circuit current of group A solar cells

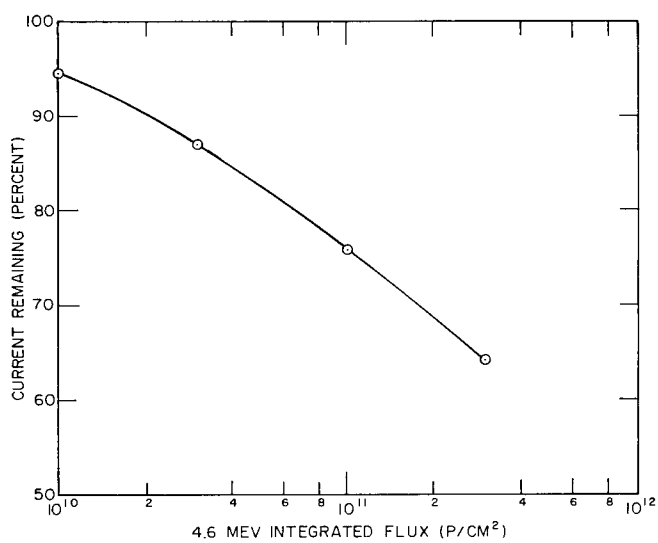

Fig. 26 - Percentage change in short-circuit current of group B solar cells

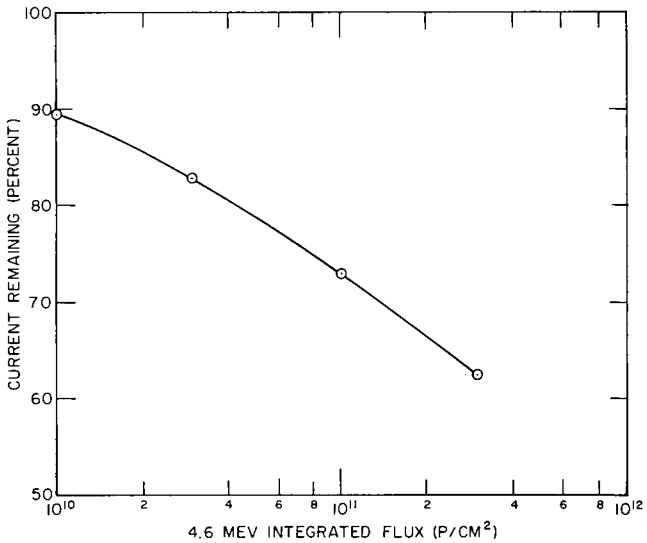

Fig. 27 - Percentage change in short-circuit current of group C solar cells

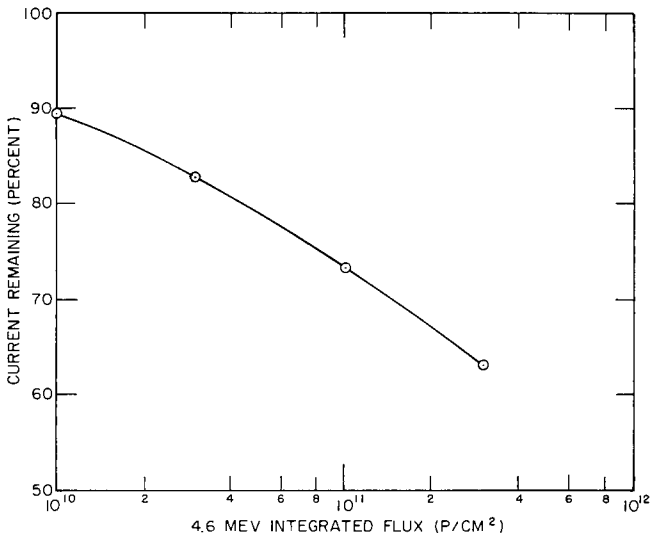

Fig. 28 - Percentage change in short-circuit current of group D solar cells

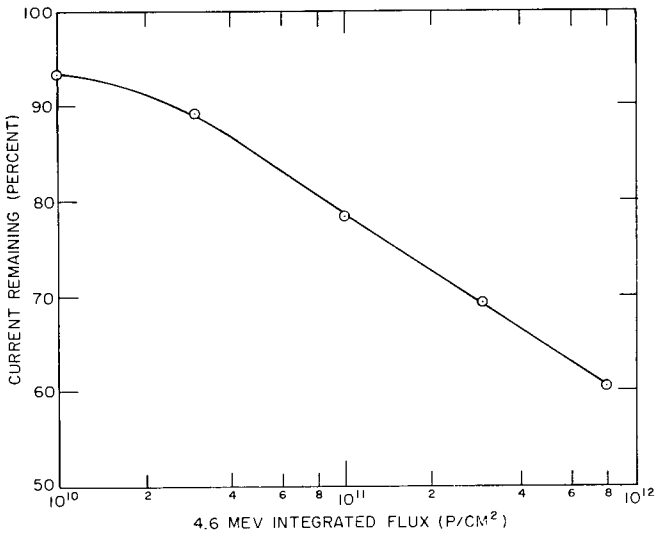

Fig. 29 - Percentage change in short-circuit current of group E solar cells

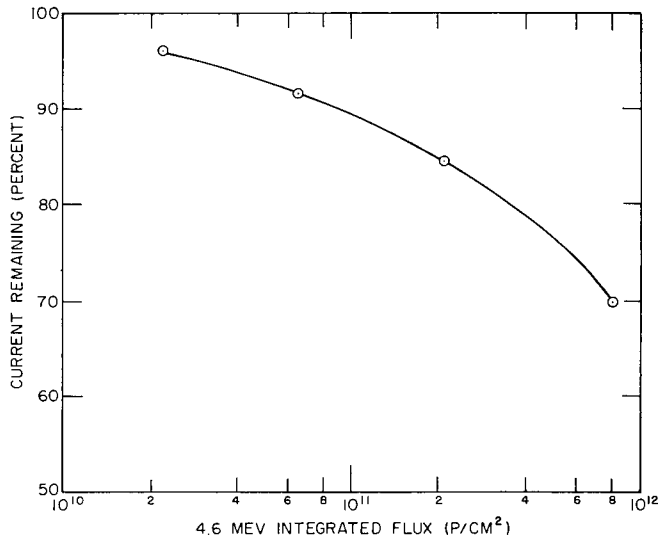

Fig. 30 - Percentage change in short-circuit current of group E_{DF} solar cells

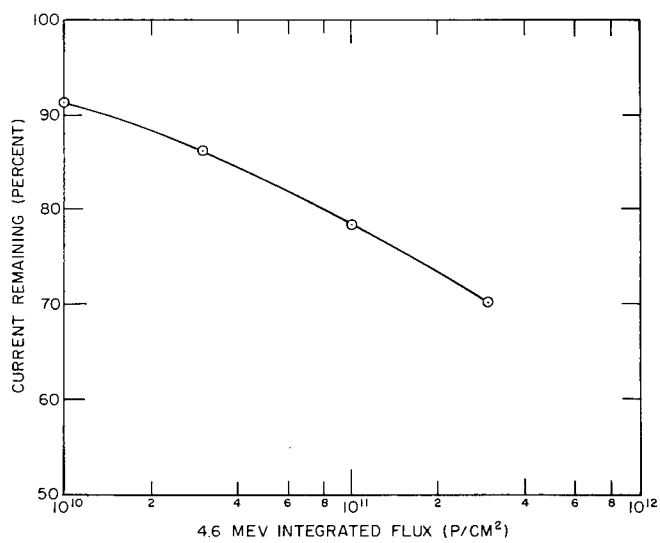

Fig. 31 - Percentage change in short-circuit current of group F solar cells

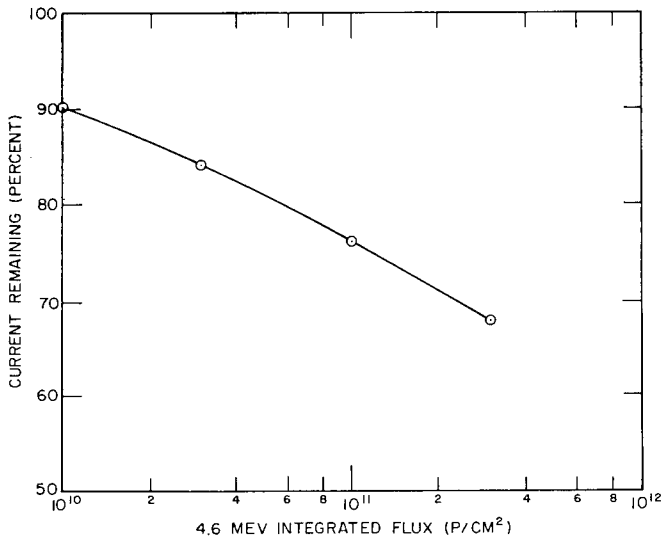

Fig. 32 - Percentage change in short-circuit current of group G solar cells

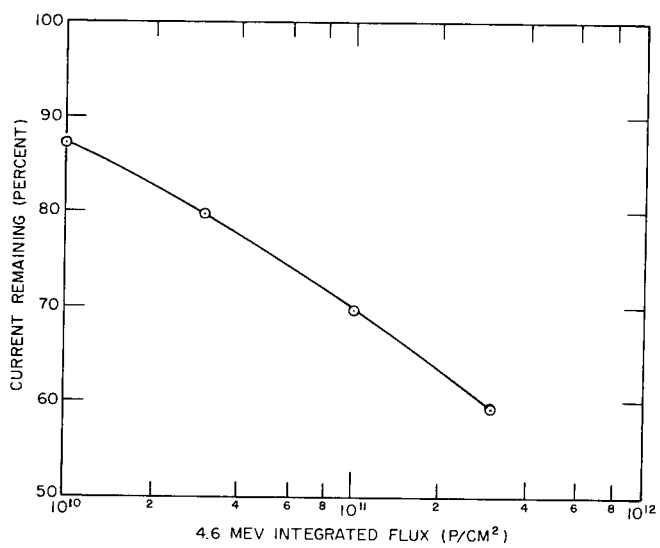

Fig. 33 - Percentage change in short-circuit current of group H solar cells

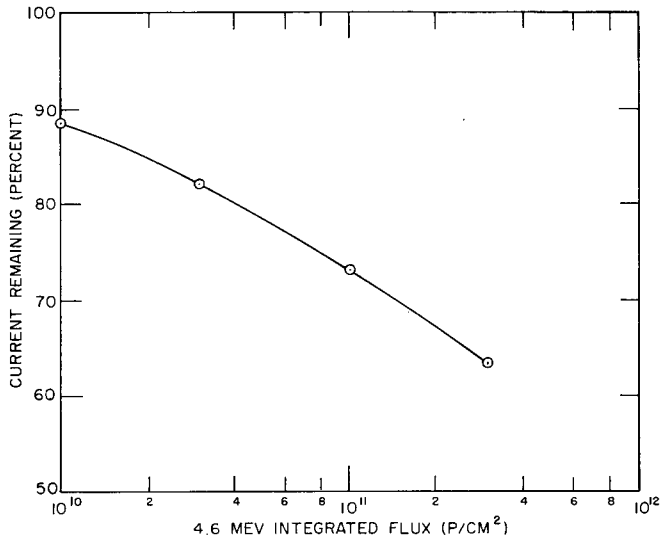

Fig. 34 - Percentage change in short-circuit current of group K solar cells

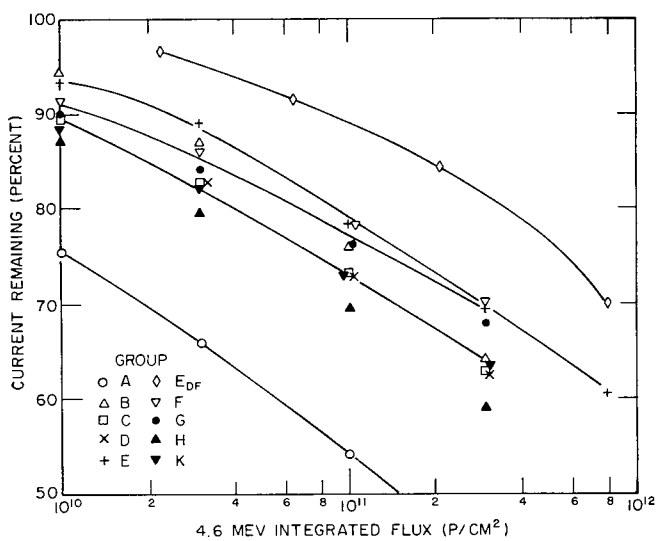

Fig. 35 - Summary of percentage change in short-circuit current of solar cells after proton bombardment

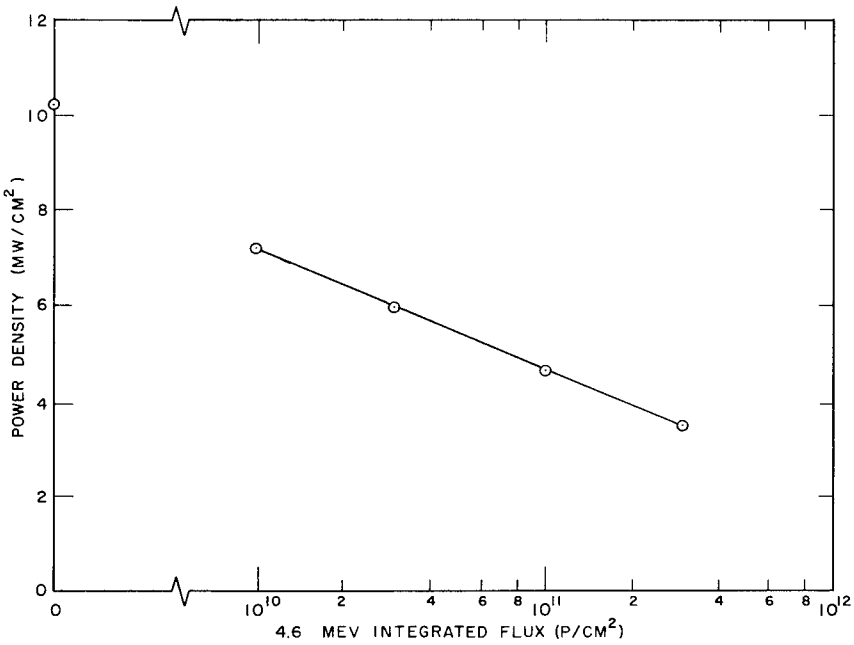

Fig. 36 - Maximum power density of group A solar cells

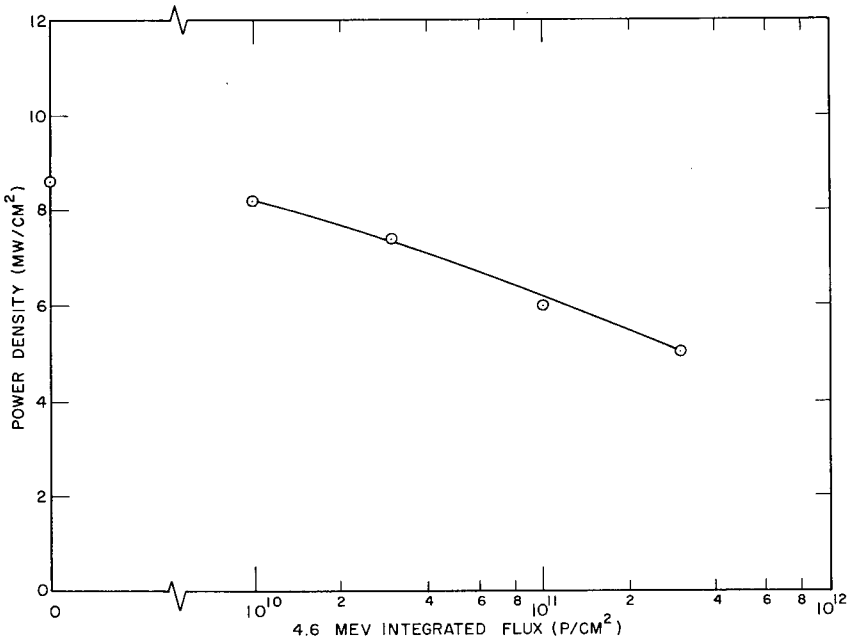

Fig. 37 - Maximum power density of group B solar cells

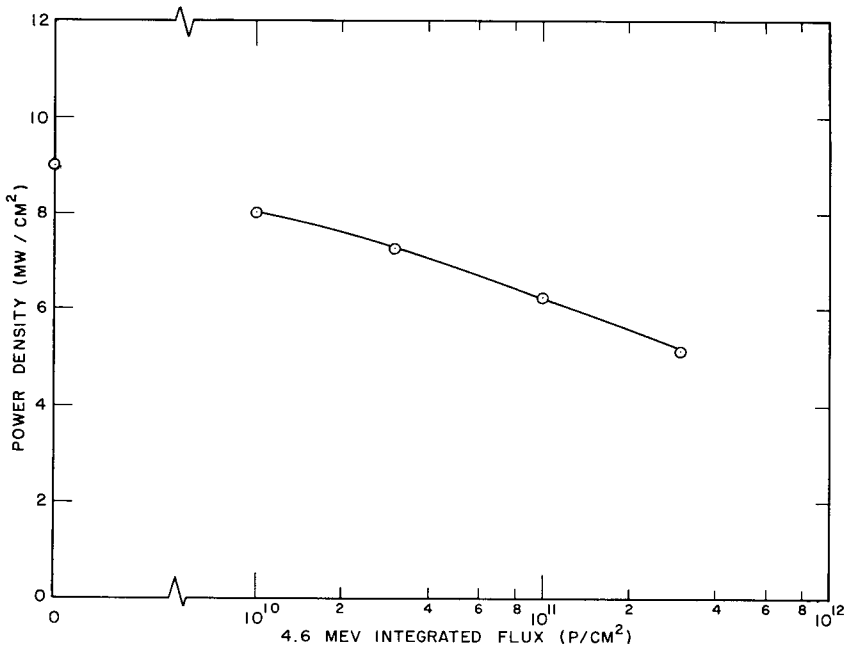

Fig. 38 - Maximum power density of group C solar cells

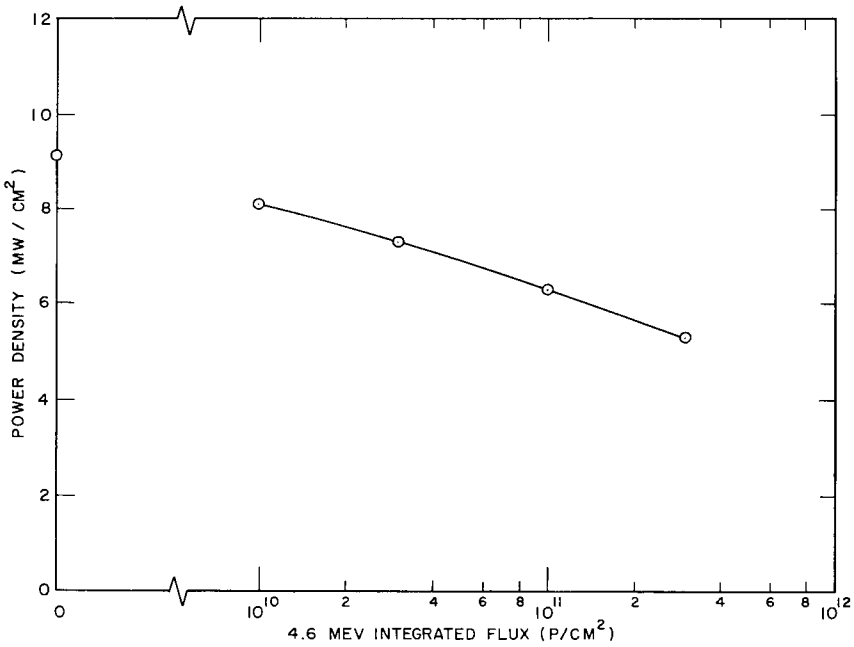

Fig. 39 - Maximum power density of group D solar cells

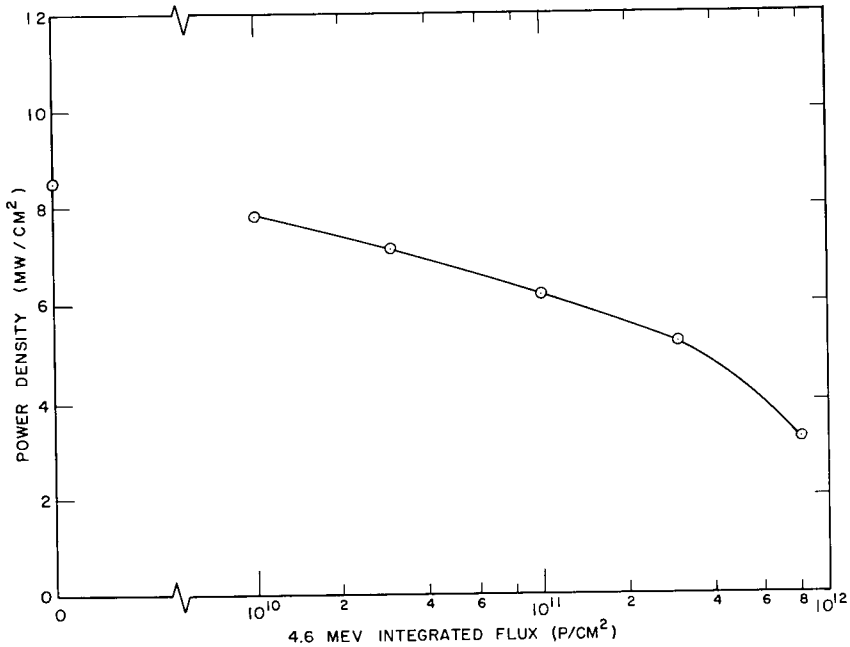

Fig. 40 - Maximum power density of group E solar cells

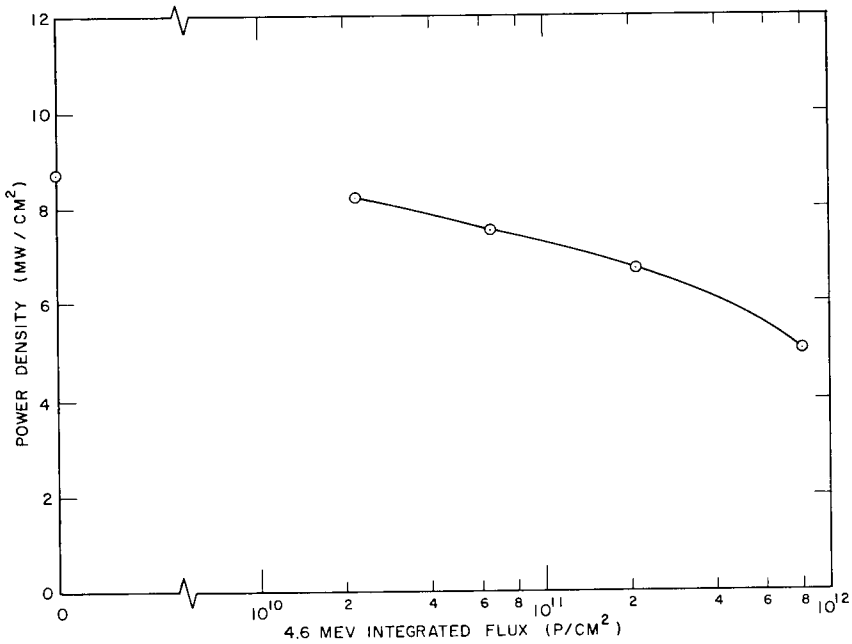

Fig. 41 - Maximum power density of group E_{DF} solar cells

UNCLASSIFIED

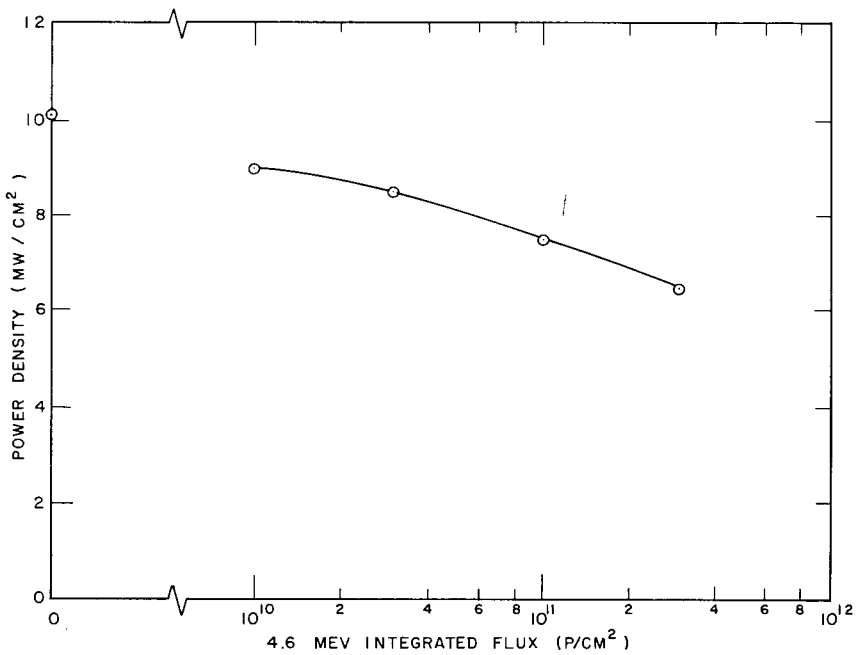

Fig. 42 - Maximum power density of group F solar cells

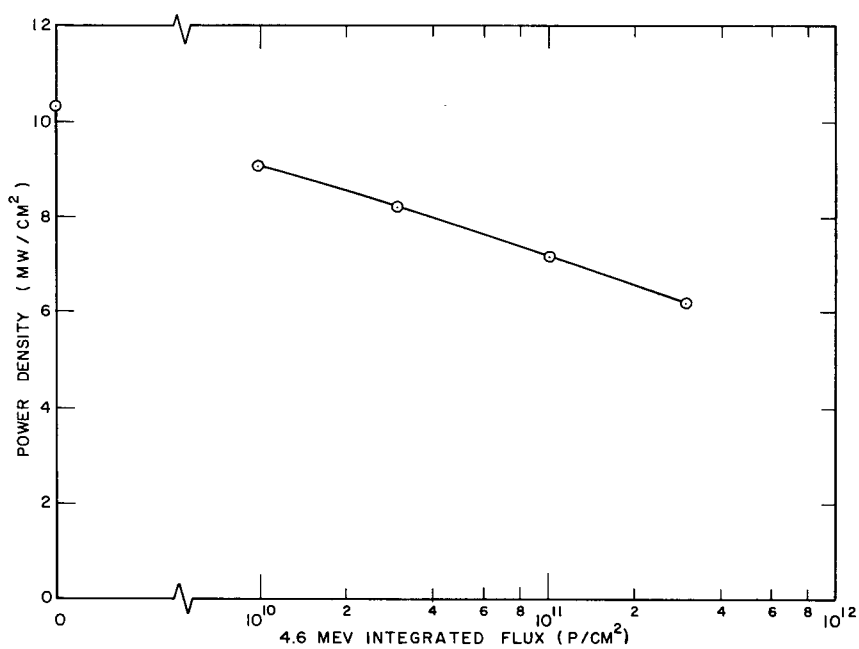

Fig. 43 - Maximum power density of group G solar cells

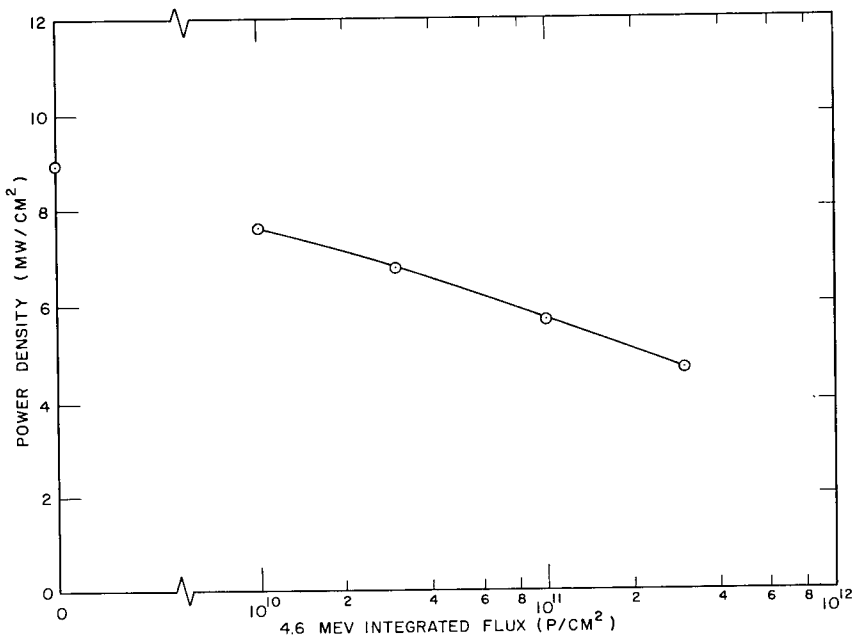

Fig. 44 - Maximum power density of group H solar cells

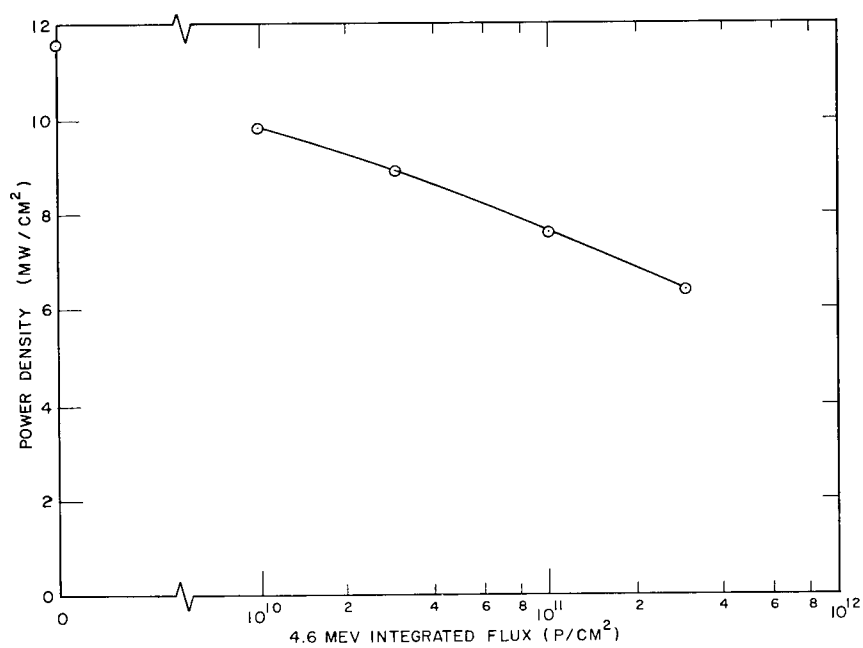

Fig. 45 - Maximum power density of group K solar cells

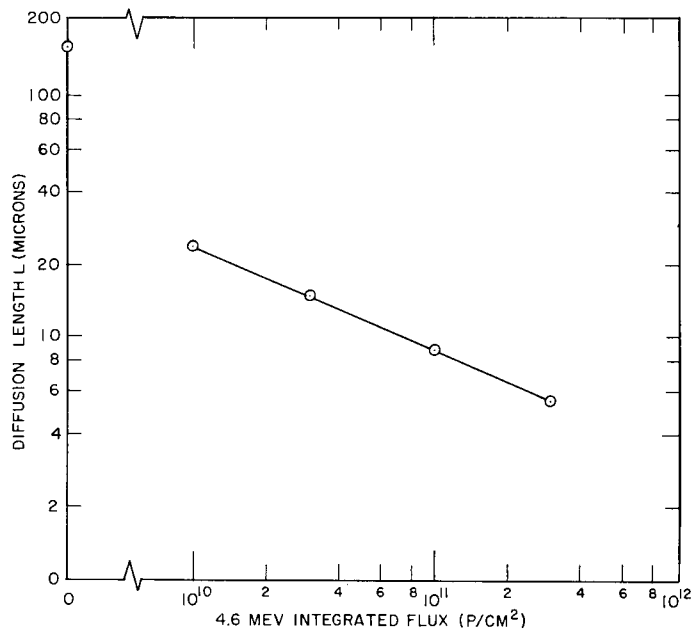

Fig. 46 - Minority-carrier diffusion length L of group A solar cells

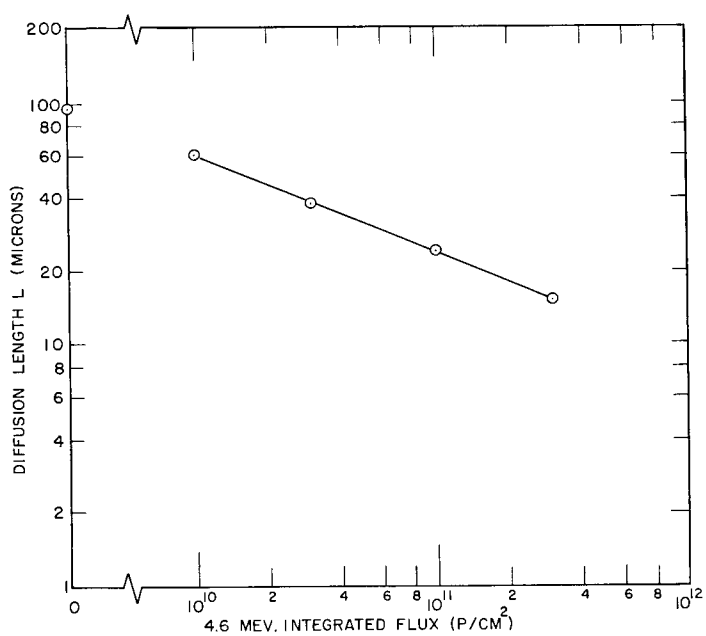

Fig. 47 - Minority-carrier diffusion length L of group C solar cells

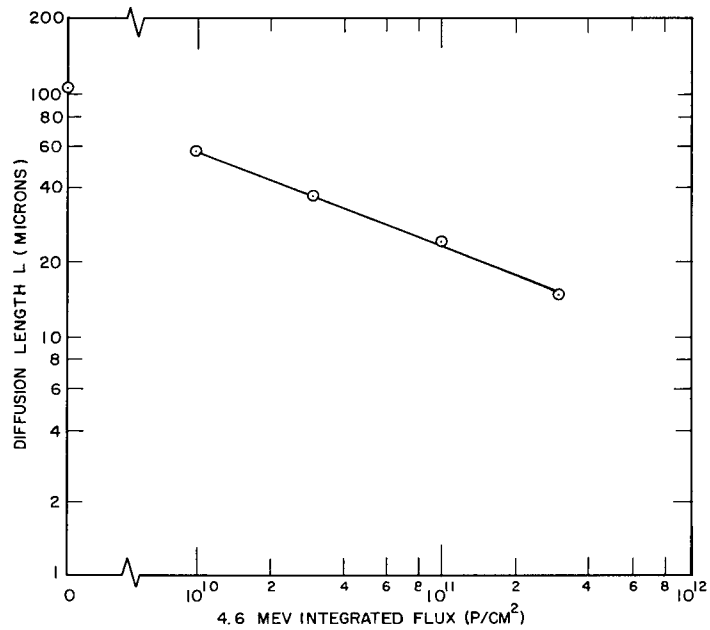

Fig. 48 - Minority-carrier diffusion length L of group D solar cells

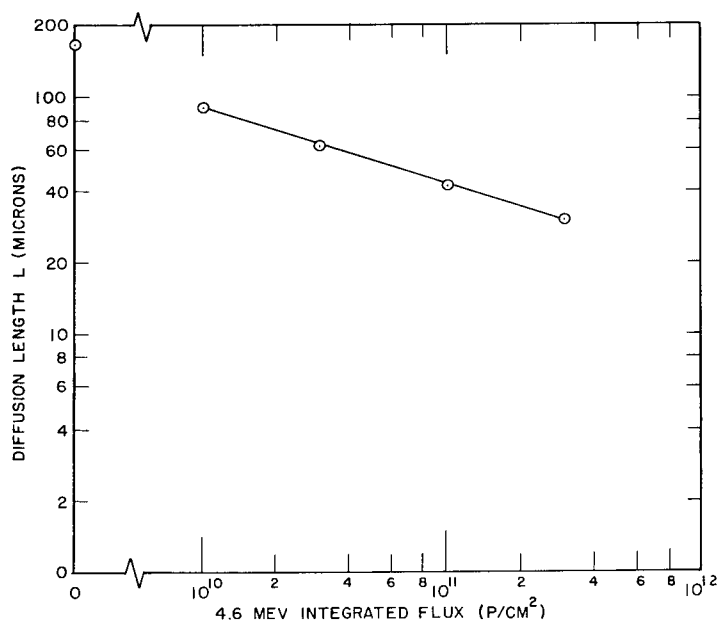

Fig. 49 - Minority-carrier diffusion length L of group F solar cells

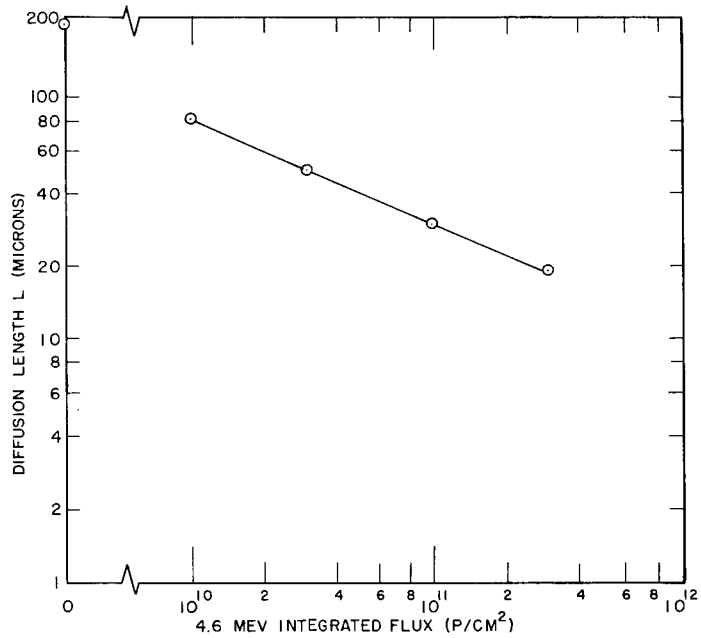

Fig. 50 - Minority-carrier diffusion length L of group G solar cells

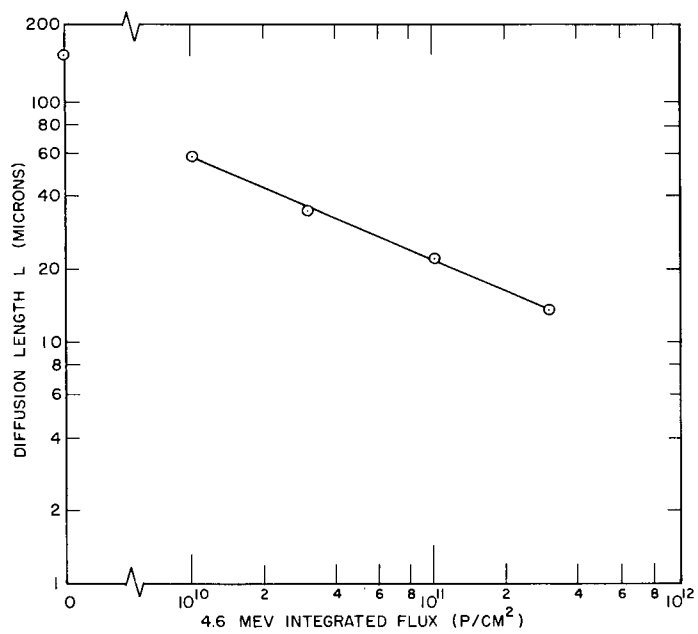

Fig. 51 - Minority-carrier diffusion length L of group H solar cells

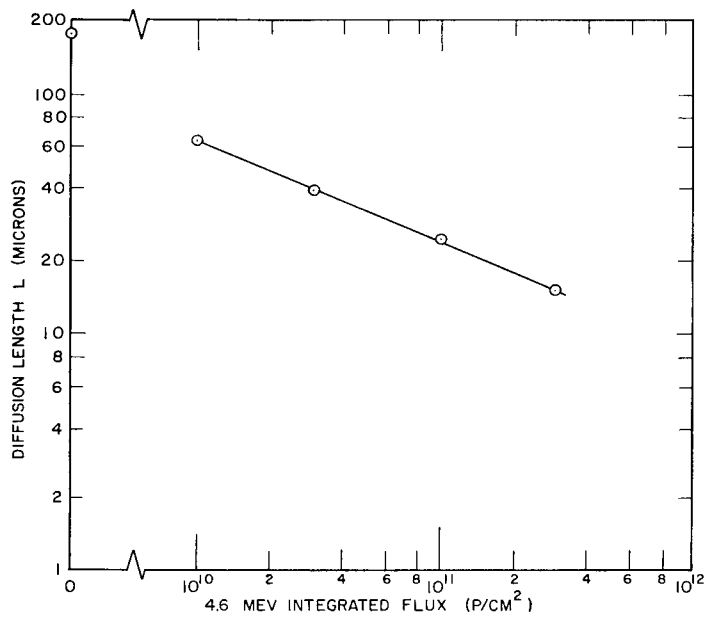

Fig. 52 - Minority-carrier diffusion length L of group K solar cells

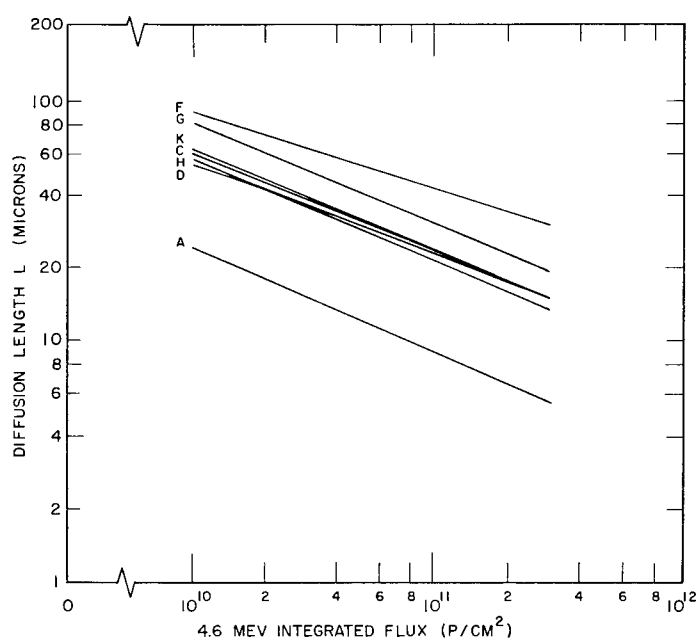

Fig. 53 - Summary of solar-cell diffusion length degradation

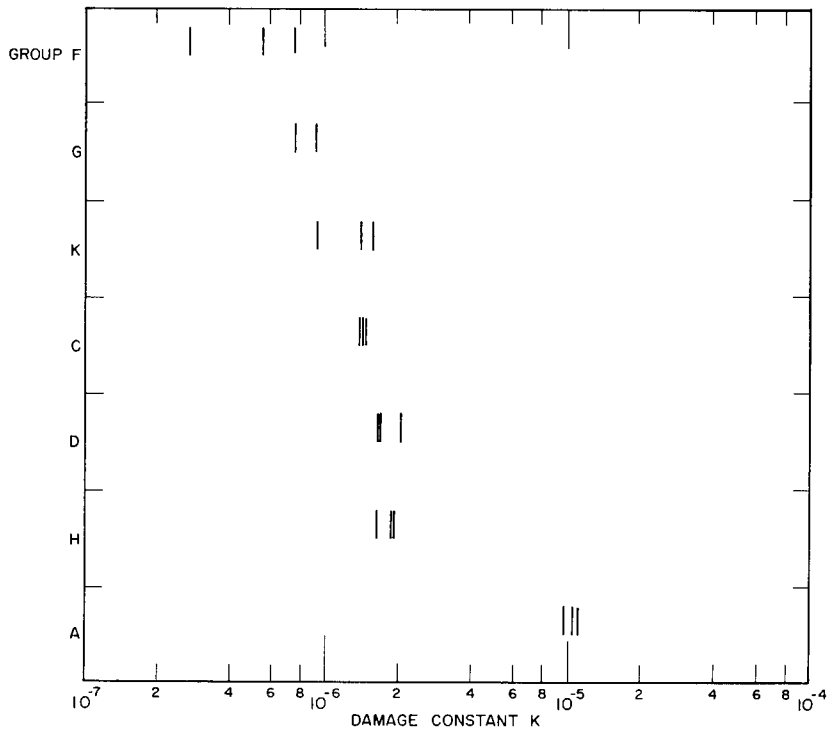

Fig. 54 - Summary of solar-cell damage constant values

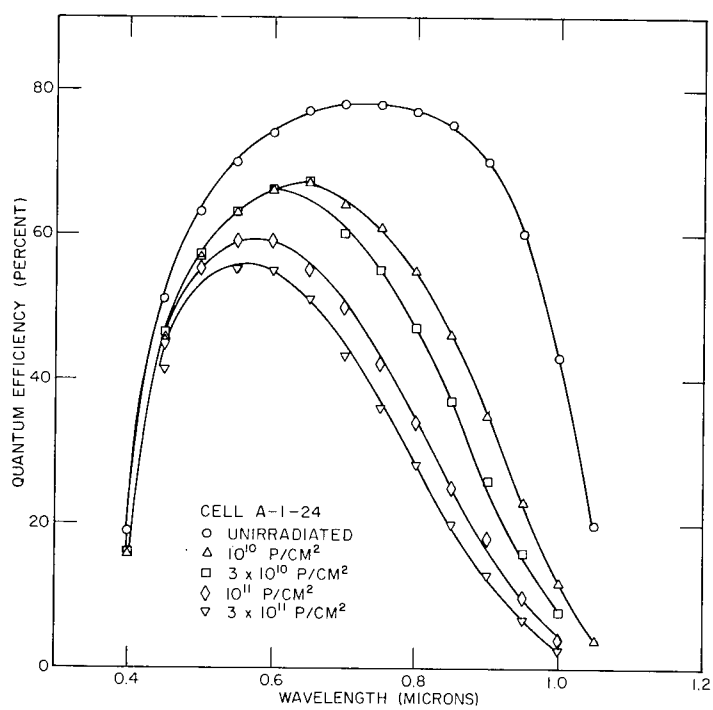

Fig. 55 - Quantum efficiency degradation of solar cell A-1-24

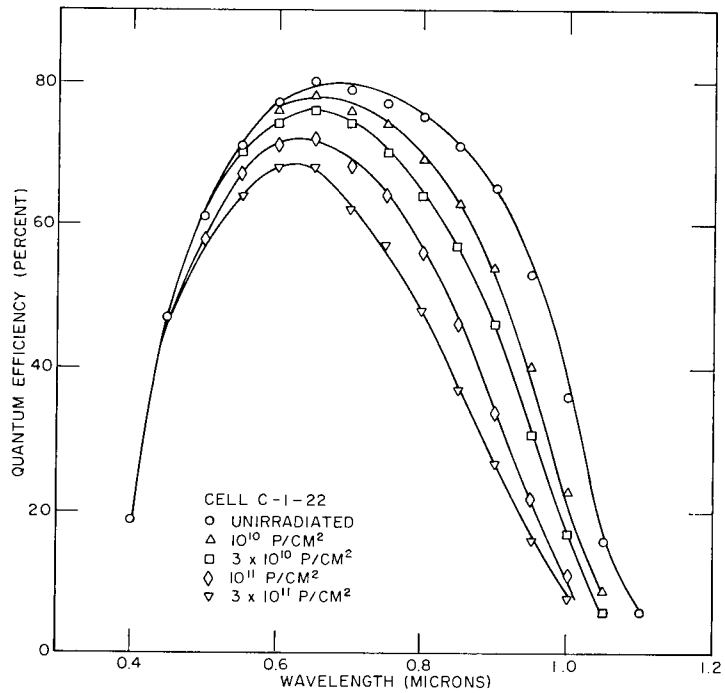

Fig. 56 - Quantum efficiency degradation of solar cell C-1-22

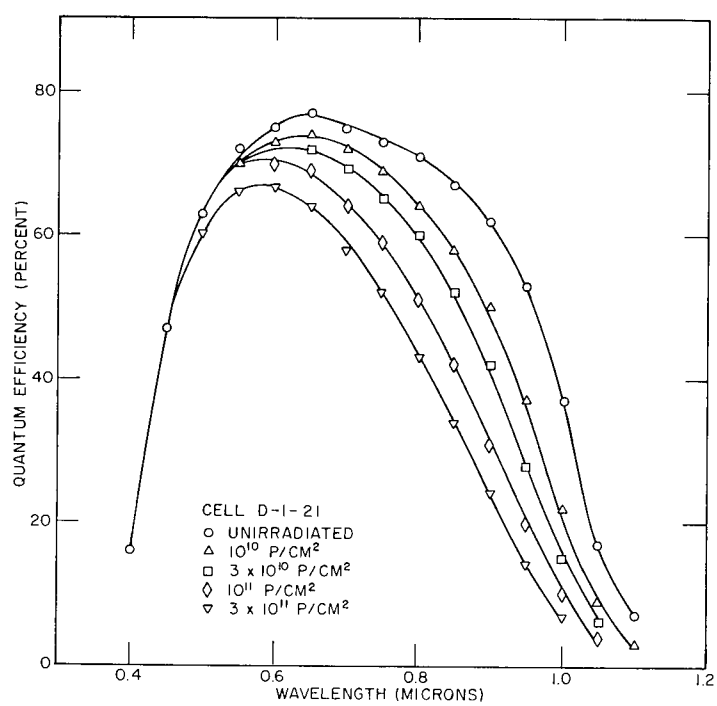

Fig. 57 - Quantum efficiency degradation of solar cell D-1-21

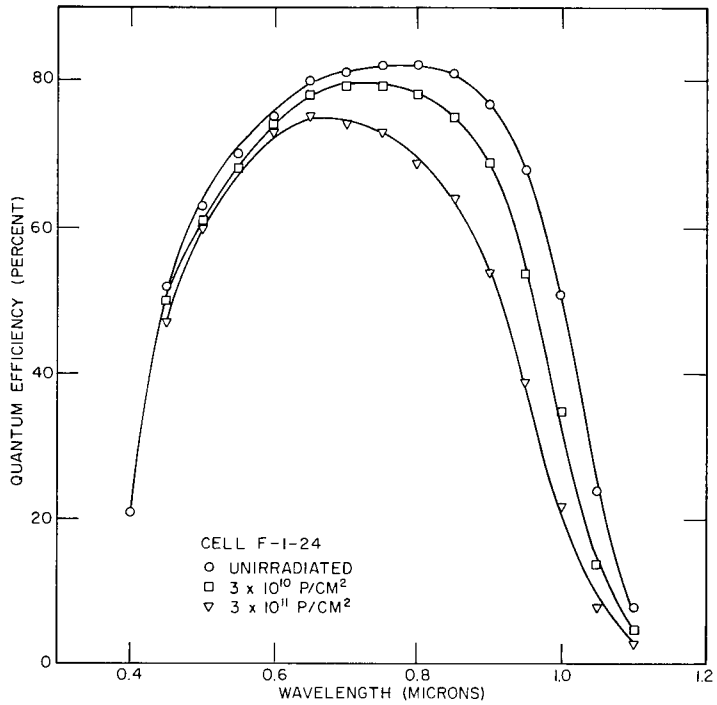

Fig. 58 - Quantum efficiency degradation of solar cell F-1-14

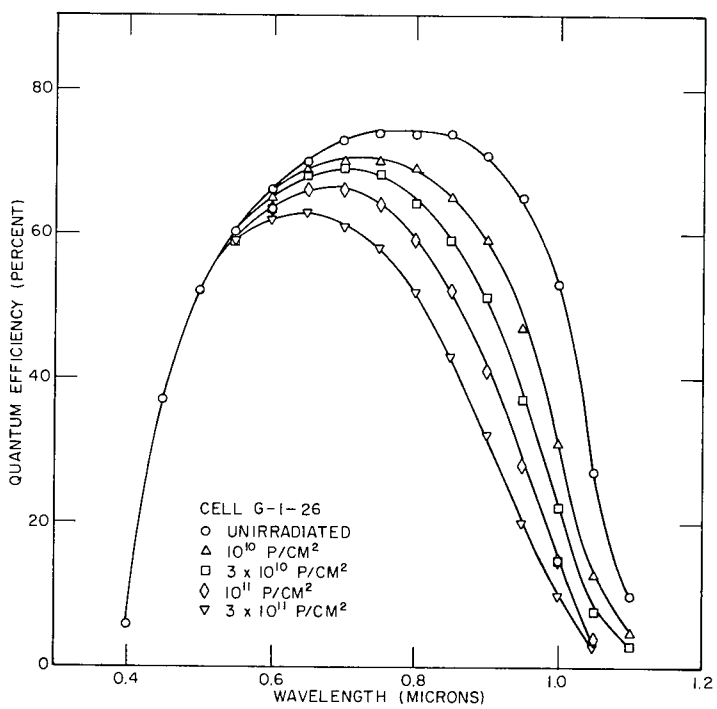

Fig. 59 - Quantum efficiency degradation of solar cell G-1-26

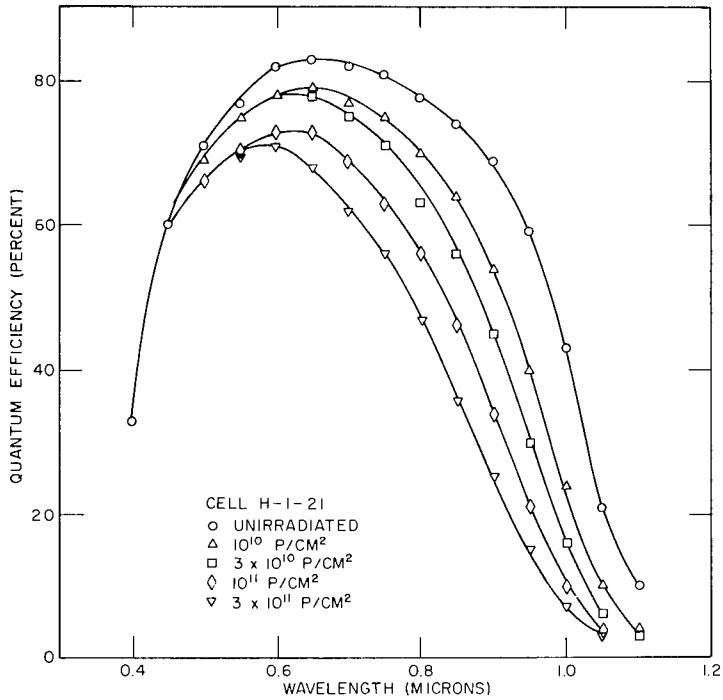

Fig. 60 - Quantum efficiency degradation of solar cell H-1-21

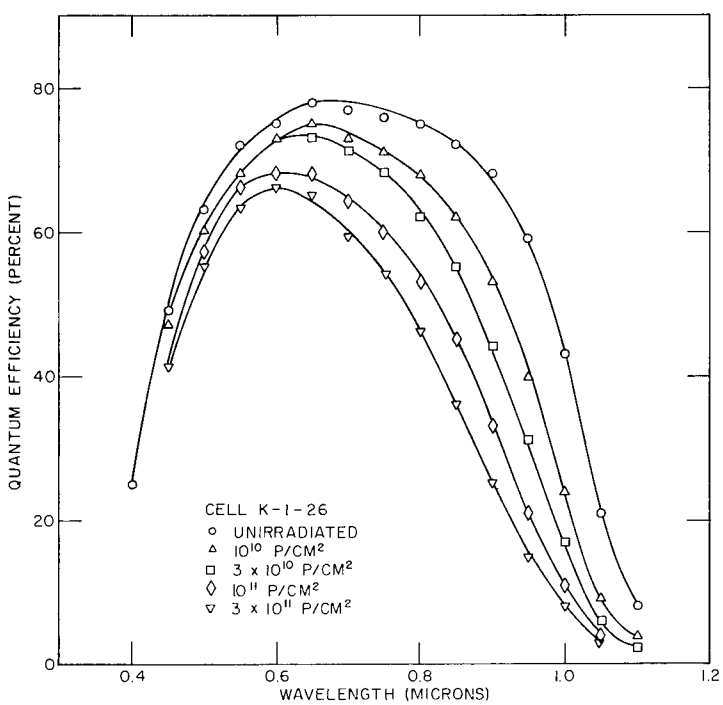

Fig. 61 - Quantum efficiency degradation of solar cell K-1-26

Unclassified

Security Classification

DOCUMENT CONTROL DATA - R&D

(Security classification of title, body of abstract and indexing annotation must be entered when the overall report is classified)

1. ORIGINATING ACTIVITY *(Corporate author)*
U.S. Naval Research Laboratory
Washington, D.C. 20390

2a. REPORT SECURITY CLASSIFICATION
Unclassified

2b. GROUP

3. REPORT TITLE
RADIATION DAMAGE IN SILICON SOLAR CELLS FROM 4.6-MEV PROTON BOMBARDMENT

4. DESCRIPTIVE NOTES *(Type of report and inclusive dates)*
A final report on one phase of the problem.

5. AUTHOR(S) *(Last name, first name, initial)*
Statler, R.L.

6. REPORT DATE
November 15, 1965

7a. TOTAL NO. OF PAGES
44

7b. NO. OF REFS
6

8a. CONTRACT OR GRANT NO.
NRL Problem E02-04

b. PROJECT NO. BuShips Projects
SF-013-12-04-4533,

c. SR-007-11-01-0549

d. NASA S-13991-G, S-4757-G

9a. ORIGINATOR'S REPORT NUMBER(S)
NRL Report 6333

9b. OTHER REPORT NO(S) *(Any other numbers that may be assigned this report)*

10. AVAILABILITY/LIMITATION NOTICES
Unlimited availability. Copies available from CFSTI – $2.00

11. SUPPLEMENTARY NOTES

12. SPONSORING MILITARY ACTIVITY
Department of the Navy (Bureau of Ships)

13. ABSTRACT

A study has been made of the radiation damage in ten types of silicon solar cells as a result of 4.6-Mev proton bombardment. The cells comprised such types as p/n cells, n/p cells with different bulk-resistivities, planar cells, and drift-field cells. A comparative analysis was made of the radiation-induced degradation in these cells as a function of short-circuit current, maximum power output, minority-carrier diffusion length, and photovoltaic spectral response. The p/n cells were found to be more sensitive to radiation damage than any type of n/p cell in this study. In the n/p cells, there is a definite trend toward increasing radiation resistance accompanying increasing values of bulk resistivity, up to 10 ohm-cm. The drift-field solar cells exhibit a further improvement in radiation resistance beyond that of the other types of n/p cells.

DD FORM 1 JAN 64 1473

Security Classification

Security Classification

14. KEY WORDS	LINK A ROLE	LINK A WT	LINK B ROLE	LINK B WT	LINK C ROLE	LINK C WT
Silicon solar cells						
Radiation damage						
Proton bombardment						
Satellites (artificial)						
Photovoltaic devices						

INSTRUCTIONS

1. ORIGINATING ACTIVITY: Enter the name and address of the contractor, subcontractor, grantee, Department of Defense activity or other organization *(corporate author)* issuing the report.

2*a*. REPORT SECURITY CLASSIFICATION: Enter the overall security classification of the report. Indicate whether "Restricted Data" is included. Marking is to be in accordance with appropriate security regulations.

2*b*. GROUP: Automatic downgrading is specified in DoD Directive 5200.10 and Armed Forces Industrial Manual. Enter the group number. Also, when applicable, show that optional markings have been used for Group 3 and Group 4 as authorized.

3. REPORT TITLE: Enter the complete report title in all capital letters. Titles in all cases should be unclassified. If a meaningful title cannot be selected without classification, show title classification in all capitals in parenthesis immediately following the title.

4. DESCRIPTIVE NOTES: If appropriate, enter the type of report, e.g., interim, progress, summary, annual, or final. Give the inclusive dates when a specific reporting period is covered.

5. AUTHOR(S): Enter the name(s) of author(s) as shown on or in the report. Enter last name, first name, middle initial. If military, show rank and branch of service. The name of the principal author is an absolute minimum requirement.

6. REPORT DATE: Enter the date of the report as day, month, year; or month, year. If more than one date appears on the report, use date of publication.

7*a*. TOTAL NUMBER OF PAGES: The total page count should follow normal pagination procedures, i.e., enter the number of pages containing information.

7*b*. NUMBER OF REFERENCES: Enter the total number of references cited in the report.

8*a*. CONTRACT OR GRANT NUMBER: If appropriate, enter the applicable number of the contract or grant under which the report was written.

8*b*, 8*c*, & 8*d*. PROJECT NUMBER: Enter the appropriate military department identification, such as project number, subproject number, system numbers, task number, etc.

9*a*. ORIGINATOR'S REPORT NUMBER(S): Enter the official report number by which the document will be identified and controlled by the originating activity. This number must be unique to this report.

9*b*. OTHER REPORT NUMBER(S): If the report has been assigned any other report numbers *(either by the originator or by the sponsor)*, also enter this number(s).

10. AVAILABILITY/LIMITATION NOTICES: Enter any limitations on further dissemination of the report, other than those imposed by security classification, using standard statements such as:

(1) "Qualified requesters may obtain copies of this report from DDC."

(2) "Foreign announcement and dissemination of this report by DDC is not authorized."

(3) "U. S. Government agencies may obtain copies of this report directly from DDC. Other qualified DDC users shall request through _____."

(4) "U. S. military agencies may obtain copies of this report directly from DDC. Other qualified users shall request through _____."

(5) "All distribution of this report is controlled. Qualified DDC users shall request through _____."

If the report has been furnished to the Office of Technical Services, Department of Commerce, for sale to the public, indicate this fact and enter the price, if known.

11. SUPPLEMENTARY NOTES: Use for additional explanatory notes.

12. SPONSORING MILITARY ACTIVITY: Enter the name of the departmental project office or laboratory sponsoring *(paying for)* the research and development. Include address.

13. ABSTRACT: Enter an abstract giving a brief and factual summary of the document indicative of the report, even though it may also appear elsewhere in the body of the technical report. If additional space is required, a continuation sheet shall be attached.

It is highly desirable that the abstract of classified reports be unclassified. Each paragraph of the abstract shall end with an indication of the military security classification of the information in the paragraph, represented as *(TS)*, *(S)*, *(C)*, or *(U)*.

There is no limitation on the length of the abstract. However, the suggested length is from 150 to 225 words.

14. KEY WORDS: Key words are technically meaningful terms or short phrases that characterize a report and may be used as index entries for cataloging the report. Key words must be selected so that no security classification is required. Identifiers, such as equipment model designation, trade name, military project code name, geographic location, may be used as key words but will be followed by an indication of technical context. The assignment of links, roles, and weights is optional.